Forschungszentrum Jülich
in der Helmholtz-Gemeinschaft

Institute of Neurosciences and Biophysics (INB)
Medicine (INB-3)

Autism and the weak central coherence theory: Investigations with functional magnetic resonance imaging

Zina-Mary Manjaly

Jül-4256

Autism and the weak central coherence theory: Investigations with functional magnetic resonance imaging

Zina-Mary Manjaly

Berichte des Forschungszentrums Jülich ; 4256
ISSN 0944-2952
Institute of Neurosciences and Biophysics (INB)
Medicine (INB-3) Jül-4256

D 82 (Diss., RWTH Aachen, 2007)

The complete volume is freely available on the Internet on the Jülicher Open Access Server (JUWEL) at http://www.fz-juelich.de/zb/juwel

Zu beziehen durch: Forschungszentrum Jülich GmbH · Zentralbibliothek, Verlag
D-52425 Jülich · Bundesrepublik Deutschland
☎ 02461/61-5220 · Telefax: 02461/61-6103 · e-mail: zb-publikation@fz-juelich.de

Hinweis zu den in dieser Dissertation enthaltenen Publikationen

Die folgenden zwei in dieser Dissertation enthaltenen Publikationen wurden in einer Auflage von jeweils mehr als 150 Stück in der Zeitschrift *NeuroImage* (herausgegeben vom Verlag Academic Press, Orlando, USA) veröffentlicht:

- Manjaly ZM, Bruning N, Neufang S, Stephan KE, Brieber S, Marshall JC, Kamp-Becker I, Remschmidt H, Herpertz-Dahlmann B, Konrad K, Fink GR (2007) Neurophysiological correlates of relatively enhanced local visual search in autistic adolescents. NeuroImage 35: 283-291.
- Manjaly ZM, Marshall JC, Stephan KE, Gurd JM, Zilles K & Fink GR (2003) In search of the hidden: an fMRI study with implications for the study of patients with autism and with acquired brain injury. NeuroImage 19: 674-683.

Die folgende in dieser Dissertation enthaltene Publikation wurde in einer Auflage von mehr als 150 Stück in der Zeitschrift *Cognitive Neuropsychology* (herausgegeben vom Verlag Taylor & Francis, London, Vereinigtes Königreich) veröffentlicht:

- Manjaly ZM, Marshall JC, Stephan KE, Gurd JM, Zilles K & Fink GR (2005) Context-dependent interactions of left posterior inferior frontal gyrus in a local visual search task unrelated to language. Cognitive Neuropsychology 22: 292-305.

To my beloved family

Table of contents

1. In search of the hidden: an fMRI study with implications for the study of patients with autism and with acquired brain injury.

This chapter contains the following publication:

Manjaly ZM, Marshall JC, Stephan KE, Gurd JM, Zilles K & Fink GR (2003)
In search of the hidden: an fMRI study with implications for the study of patients with autism and with acquired brain injury.
NeuroImage 19: 674-683.

1.1 Summary

The Embedded Figures Task involves search for a target hidden in a more complex visual pattern. The task has been used to study local perception and visual search in a range of normal and pathological populations. After acquired brain damage, impairment on embedded figures is strongly associated with aphasia; in the context of developmental disorder, people with autism or with Asperger's syndrome are reliably found to be better than normal controls on the task. The current study employed functional MRI with healthy volunteers to elucidate the brain regions that are specifically involved in the local search aspects of the Embedded Figures Task. We did so by analyzing the neural activations that are implicated in the task over and above those involved in an easier visual search task and in a straightforward shape recognition task. Significant activations ($p<0.05$, corrected) specific in the above sense to the Embedded Figures Task were found in left inferior and left superior parietal cortex and in left ventral premotor cortex (inferior frontal gyrus). By contrast, comparing the overall effect of visual search within geometric figures to pure recognition of geometric shapes revealed more widespread activations in parietal, occipital, cerebellar, and frontal areas bilaterally. The implications of these findings for some developmental and acquired pathologies of perceptual functioning are

outlined. We also relate our results to studies of local / global processing in other tasks.

1.2 Introduction

The Embedded (or hidden) Figures Task was originally devised by Gottschaldt (Gottschaldt, 1926) in order to study the “influence of past experience upon the perception of visual forms”. His findings, however, indicated that the frequency and recency of seeing the target shape had little effect upon the ease of finding that shape when embedded in a more complex figure. Much subsequent work accordingly investigated how the structural properties of the target and complex figure influenced search times and error rates on the task (Gottschaldt, 1929; Reed and Angaran, 1972).

Clinical studies that have deployed the Embedded Figures Task have typically done so to investigate the processes of local perception and visual search. In a population of men with penetrating missile injury to the brain, Teuber and Weinstein (Teuber and Weinstein, 1956) showed that impairment on the task could follow injury to any lobe of the brain (frontal, parietal, temporal, and occipital) in either cerebral hemisphere. More interestingly, patients with aphasia were significantly more impaired than non aphasic brain-injured patients, who were in turn more impaired than control subjects. This somewhat unexpected association with aphasia was replicated by Russo and Vignolo (Russo and Vignolo, 1967) and Orgass, Poeck, Kerschensteiner and Hartje (Orgass et al., 1972). No convincing explanation for the association between aphasia and impaired performance on embedded figures has yet been forthcoming. Teuber and Weinstein (Teuber and Weinstein, 1956) suggested that the result may be an artifact of differential severity of brain damage, but ratings of this latter variable in the study of Orgass et al. (Orgass et al., 1972) are

not consistent with this speculation. Furthermore, all the relevant studies took care that the task instructions were understood by the aphasic patients.

More recently, interest in the Embedded Figures Task has been sparked by the discovery that subjects with autism or with Asperger's syndrome are better at the task than matched control subjects (Shah and Frith, 1983; Happé, 1999). Furthermore, the parents of children with Asperger's syndrome are also faster on the task than non-autistic adult controls who do not have children with Asperger's syndrome (Baron-Cohen and Hammer, 1997).

It is thus of considerable clinical importance to ascertain which brain regions are implicated in the critical and distinctive aspects of the Embedded Figures Task. Functional neuroimaging might provide this information. There is one published study of the cerebral correlates of the task using functional MRI (Ring et al., 1999). That experiment (which included autistic subjects and matched controls) contrasted the Embedded Figures Task with a control condition in which subjects were required "to fixate on a blank screen". This design yielded (for the control and autistic groups combined) many significant activations that covered frontal, parietal, temporal, and occipital cortex in both hemispheres. The current fMRI study accordingly seeks to discover which of these brain regions are specifically involved in the Embedded Figures Task when compared to both a closely related but easier visual search task and a high-level baseline (a straightforward shape recognition task).

1.3 Material and methods

1.3.1 Subjects

Sixteen healthy, right-handed male volunteers (aged 20 to 36 years; mean age 24.3 years ± standard deviation 4.3 years) with no history of neurological or psychiatric illness were studied. We employed only men because of the known sex ratio in

autism: between 3:1 and 10:1, with the higher incidence in males (Happé 1994). Furthermore, restricting the choice of subjects to males avoided the normal variation in brain size and shape between the two sexes and hence improved image normalization (see Image Processing). The study was approved by the local ethics committee. Informed consent according to the Declaration of Helsinki was obtained prior to participation for all participants.

1.3.2 Stimuli and experimental design

Following behavioural pilot testing, we devised our own version of the Embedded Figures Task (EFT) to ensure that (i) the stimuli matched the display properties in the MR scanner, and (ii) to ensure that mean error rates on the EFT did not exceed 15% and mean errors on the CT did not exceed 5% when the stimuli were displayed for 3000 ms. It is crucial to the design of this experiment that the control task is easier than the experimental task. All custom made stimuli were produced using a PC graphics program (Corel Draw 9.0, Corel Corp). 32 geometrical figures with an identical number of composing lines (12) and comparable complexity were created. Each of these complex figures was presented eight times throughout the course of the experiment: four times in the EFT conditions (C1, C2; see below) and four times in the CT conditions (C3, C4; see below). In all conditions, each complex figure was accompanied by a simple target figure. These target figures were either embedded into the simultaneously presented complex figures (50% of trials) or were not part of any of the complex figures shown on any trial (50% of trials). Each correct target figure was only shown once throughout the entire experiment to minimize priming effects. Since the incorrect target figures were not embedded in any of the complex figures used in the experiment, they could safely be used twice, i.e. once in each task.

Figure 1 shows examples of the as stimuli used during EFT and the CT, and also depicts the design of the experiment. The critical conditions of this factorial design are conditions 1 and 2 (Factor 1: task, level: EFT) in which subjects were presented on each trial with one target figure and one more complex figure in which the target was or was not embedded (C1: horizontal presentation of the two figures; C2: vertical presentation of the two figures). Subjects were instructed to indicate via right hand button presses whether or not the target was embedded in the complex figure. Subjects pressed one button with their index finger if the answer was 'yes' and another button with their middle finger if the answer was 'no'. In conditions 3 and 4 (Factor 1: task, level: CT), subjects were presented with the same stimuli which were, however, disambiguated: i.e. a figure within the complex figure was highlighted (C3: horizontal presentation of the two figures; C4: vertical presentation of the two figures). Subjects were instructed to indicate via right hand button presses whether or not the target figure matched the figure highlighted within the complex figure. Subjects pressed one button with their index finger if the answer was 'yes' and another button with their middle finger if the answer was 'no'.

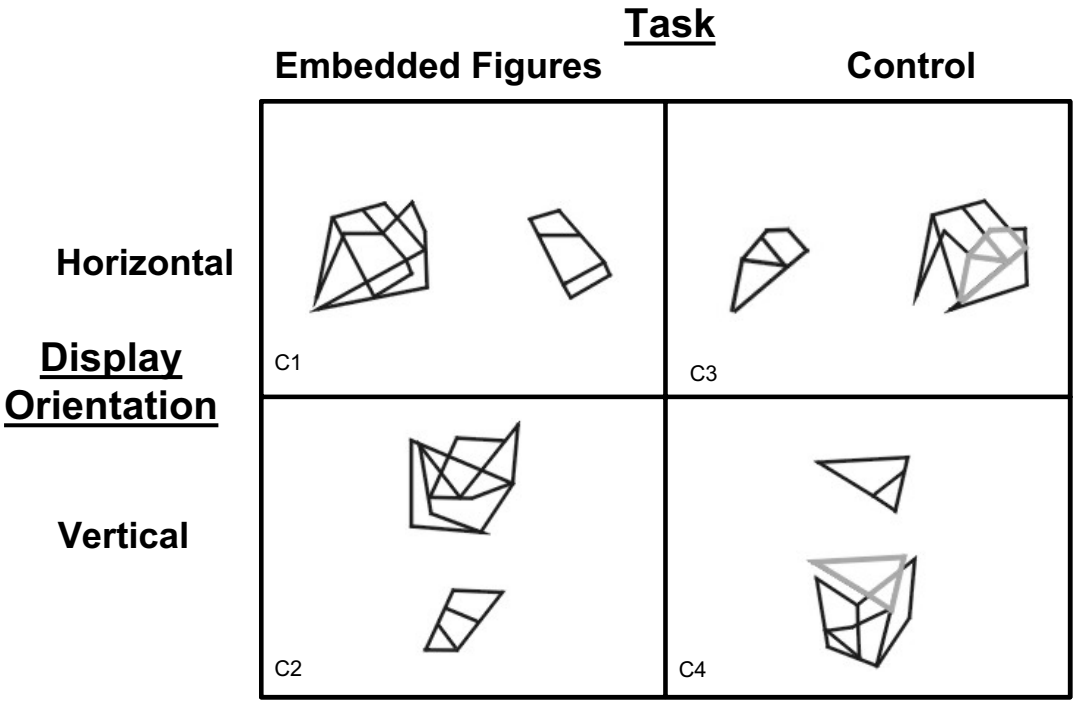

Figure 1: Stimuli and study design. Examples of the stimuli used for the Embedded Figures Task (EFT) and the control task (CT). Stimuli were displayed either horizontally or vertically. In the EFT subjects judged whether the target figure was or was not embedded in the more complex figure. In the CT subjects judged whether the target figure did or did not match the highlighted figure (indicated in gray) within the complex figure.

Comparing conditions 1 and 2 (EFT) with conditions 3 and 4 (CT) should reveal the specific neural correlates underlying the search for an embedded (hidden) figure. Factor 2 (display orientation, conditions 1 and 3: horizontal, conditions 2 and 4: vertical) was introduced for the following reasons: this factor allows the identification of areas which respond to searching for an embedded figure, regardless of display orientation, i.e. irrespective of the actual spatial layout. Furthermore, the assessment of the interaction term should reveal whether or not display orientation has a differential effect on the neural activity resulting from searching for the target in a complex figure versus a more simple visual search task (i.e. the control task employed here).

During the fMRI measurements, stimuli were presented in black on a white background on a 16 x 8.4 cm screen (horizontal visual angle of 34°, vertical visual

angle of 18º) for 3000 ms (stimulus on-time, SOT) with an interstimulus interval (ISI) of 1000 ms (blank screen) using Presentation 0.43 (Neurobehavioral Systems Inc., San Francisco). Subjects viewed the display from a distance of 26 cm (14 cm screen to mirror, 12 cm mirror to subjects´ eyes). In conditions 1 and 3, stimuli corresponding to visual angles of 8º x 8º were presented horizontally left and right of the center of the screen. In 50% of the trials the target appeared to the left of the display center and the complex figure appeared right to the display center. In the other 50% of the trials these positions were reversed. Each stimulus was presented at a horizontal eccentricity of 7º to the medial border of the stimulus. In conditions 2 and 4, stimuli corresponding to a visual angle of 8º x 8º were presented above and below the center of the display. In 50% of the trials the target appeared above the center and the complex figure below the center. In the other 50% of the trials these positions were reversed. Each stimulus was presented at a vertical eccentricity of 0.4º to the stimulus border closest to the center of the display screen. That the horizontal and vertical eccentricities were different from each other was necessitated by the spatial restrictions of the display screen in the scanner. We controlled for order effects by (i) counterbalancing the condition order within subjects (i.e. across runs) and between subjects using four different block sequence patterns, and (ii) randomizing the order of stimuli across blocks of trials and conditions. In a block of trials a total of 8 stimuli were shown, hence each condition lasted 32 sec.

Between conditions, a high-level “baseline” (lasting 24 sec) was implemented, in which subjects viewed squares or triangles presented centrally. SOT and ISI matched those used in the experimental conditions. Subjects were instructed to indicate via right hand button presses whether or not the figure presented was a square. Subjects pressed one button with their index finger if the answer was ‘yes’ and another button with their middle finger if the answer was ‘no’. This shape

recognition task controlled for visual recognition and attention, decision-making and response processes but did not involve visuospatial search. In addition, this baseline condition helped to ensure that the same cognitive state preceded all experimental conditions. Before the beginning of each baseline condition, instructions were displayed visually for 4 sec. After each baseline condition, instructions of the subsequent task were given for 4 sec: These instructions informed the subject whether he had to perform the EFT or the CT, and whether the stimuli were arranged horizontally or vertically.

Reaction times of the button presses (measured from stimulus on-set) and error rates were recorded as measures of task difficulty and task performance. Subjects were instructed to respond as quickly as possible after they were convinced of the accuracy of their decision. In all conditions (both the experimental conditions of interest and the high-level baseline), the number of correct 'yes' and 'no' responses was 50% each. All subjects' condition-specific mean reaction times and mean error rates of all four experimental runs were compared by analysis of variance (ANOVA, repeated measures), using SPSS V9 (SPSS Inc., Chicago, IL).

1.3.3 Eye movements and eye movement data analysis

All tasks (EFT, CT, high-level baseline task) were performed in free vision for the following reasons: First, the clinical version of the EFT is thus performed. Second, the EFT becomes much more difficult when eye movements are disallowed. Third, we did not wish to introduce an additional spatial constraint by making the subjects fixate at the center of the screen: it has previously been demonstrated that there is a strong interaction between the neural activity resulting from a visuospatial attention task and allowing / disallowing eye movements (Fink et al. 1997a).

As the tasks were undertaken in free vision, we recorded eye movements in all subjects during the MR measurements to assess whether differential eye movements occurred in the EFT and control conditions. For the purpose of on-line monitoring of eye positions relative to the screen and the stimuli thereon, an infrared video-based eye-tracking device (ASL 504, fitted with a long-distance optics module; Applied Science Laboratories, Bedford, MA, USA) was used. Eye movement data were analyzed by the open source software ILAB (Gitelman et al., 2001) and MATLAB 5.3 (The Mathworks Inc., Natick, MA, USA).

After removal of eye blink artefacts, the data were analyzed for the presence of systematic changes in eye position. Eye position was analyzed using the normalized x- and y- coordinates of the subject's gaze on the screen. For each of the four experimental conditions (and the high-level baseline), the data were analyzed for the length of the total scan path and the overall time that subjects kept their gaze in the proximity of the visual stimuli. For each subject, eye movement measurement epochs were averaged across all corresponding stimulus locations and separately across all target stimuli during each condition period. The subjects' mean values of each experimental condition were compared by ANOVA using SPSS V9 (SPSS Inc., Chicago, IL).

1.3.4 MRI acquisition

The entire brain was scanned in 3D to obtain anatomical images using a high-resolution, T1-weighted MP-RAGE pulse sequence (magnetisation-prepared, rapid acquisition gradient echo) with the following parameters: TR (repetition time) = 11.4 ms; TE (echo time) = 4.4 ms; q (flip angle) = 15°; 1 excitation; field-of-view (FOV) = 230 mm; matrix = 200 x 256; 128 sagittal slices with 1.41 mm slice thickness. Echo Planar Imaging (EPI) was performed on a Magnetom Vision 1.5 Tesla scanner

(Siemens Medical Systems GmbH, Erlangen, Germany) equipped with a gradient booster system; the standard head coil was used for radiofrequency transmission and signal reception. Pulse sequence parameters were as follows: gradient echo EPI; TE = 66 ms; TR = 4s; FOV = 200 x 200 mm; q = 90°; matrix size = 64 x 64; pixel size = 3.125 x 3.125 mm; slice thickness = 4.0 mm; inter-slice gap = 0.4 mm; 30 slices. Since our EPI sequence triggered data acquisition for each slice individually, the data were scaled to ensure inter-slice, intra-volume comparability of the raw signal intensities.

The blocked design fMRI paradigm, which was preceded by 4 dummy scans to allow the MR signal to reach a steady state, comprised 8 repetitions of the 24s high level baseline (6 TR) and an 32s activation state (8 TR). Thus, during the activation state, 8 whole-brain images were acquired and during the high-level baseline state 6 whole-brain datasets were acquired, separated by instruction blocks of four seconds (1 whole-brain data set). A blocked design was adopted in preference to an event-related approach in order to maximize efficiency, that is, to maximize the variance that the explanatory factors account for. Also, the search processes were likely to vary in duration thus leading to uncertainties with regard to the timing of the cognitive of interest apart from those processes concerned with stimulus onset. Each volunteer performed 4 repetitions of the experiment (with counterbalanced condition order within and across subjects) during the complete measurement procedure.

1.3.5 Image processing

All calculations and image manipulations were performed on Sun Ultra 60 workstations (SUN Microsystems Computers) using MATLAB 5.3 (The Mathworks Inc., Natick, MA, USA) and SPM99 (Statistical Parametric Mapping software, SPM; Wellcome Department of Cognitive Neurology, London, UK;

http://www.fil.ion.ucl.ac.uk). SPM was used for image realignment, co-registration of structural and functional images, image normalization, smoothing, and to create statistical maps of significant relative regional BOLD response changes (Friston et al., 1995a; Friston et al., 1995b).

The first four images of each time-series, during which the MR signal reaches a steady-state, were discarded. The remaining 128 volume images of each time-series were automatically realigned to the first image (corresponding to the 5th acquired image of the time series) to correct for head movement between scans. Image sets of the four conditions and the baseline were then co-registered to the 3D anatomical data set and transformed into a standard stereotactic space (Talairach and Tournoux, 1988). The space of the template images used in SPM for image normalization is based upon the Talairach system but derived from 152 brains at the Montreal Neurological Institute; see the SPM templates manual for details. This spatial transformation includes both linear and non-linear components and uses a non-linear sampling algorithm (Friston et al., 1995a). Data were thereafter expressed in terms of standard stereotactic coordinates in the x-, y- and z-axes (as defined in Table 1). The resulting pixel size in standard stereotactic space was 2 x 2 x 2 mm. Transformed functional data sets from each subject were smoothed with a Gaussian kernel of 10 mm (full width half maximum) for the group analysis to meet the statistical requirements of the “General Linear Model” and to compensate for normal variation in individual brain size, shape and sulcal / gyral anatomy across subjects.

1.3.6 Statistical analysis

Following stereotactic normalization and smoothing, statistical analysis was performed. Subject-specific low frequency drifts in signal were removed by a high pass filter of 132 sec. Thereafter, global means were normalized by proportional

scaling. Data were analyzed modeling the different conditions as reference waveforms (i.e. box car functions convolved with a haemodynamic response function in the context of the general linear model employed by SPM99). For each subject, we accordingly defined a design matrix modeling the alternating periods of experimental conditions using a delayed box-car reference vector that accounted for the delayed cerebral haemodynamic response function after stimulus presentation. Additionally, for each experimental run, we included twelve parameters obtained from the realignment procedure as additional regressors in the design matrix. These regressors consisted of six absolute and six differential parameters describing rotation and translation of the subject's head during the experiment. After estimation of all model parameters, specific effects were tested by applying appropriate linear contrasts to the parameter estimates for each condition, resulting in a t-statistic for each and every voxel. These t-statistics (transformed to Z-statistics) constitute a subject-specific statistical parametric map ($SPM_{\{z\}}$). The $SPM_{\{z\}}$ were then interpreted by referring to the probabilistic behavior of Gaussian random fields. In all analyses, areas of activation were identified as significant only if they passed a threshold of $p_c < 0.05$, corrected for multiple comparisons at the cluster level (Friston et al., 1995b).

For each subject, we first determined the overall effect of visual search in geometric figures relative to pure recognition of geometric shapes by contrasting the mean parameter estimate across all visual search conditions to that of the high-level baseline (i.e. ¼ [C1 + C2 + C3 + C4] > baseline). In subsequent analyses, the main effects of *task* (i.e. C1 + C2 > C3 + C4, and C3 + C4 > C1+ C2) and *display orientation* (i.e. C1 + C3 > C2 + C4, and C2 + C4 > C1 + C3) were assessed. In these analyses, C1 + C2 > C3 + C4 (and vice versa) and C1 + C3 > C2 + C4 (and vice versa) were masked with C3 + C4 > baseline (and C1 + C2 > baseline) and C2 + C4 > baseline (and C1 + C3 > baseline), respectively, to assess whether or not

relative increases in neural activity reflected activations of one condition or rather deactivations of the other (relative to the high-level baseline). In addition, the data were analyzed for the interaction of *task* and *display orientation*.

For the fMRI data group analysis, the contrast images from the analysis of the individual subjects were analyzed by one sample t-tests (using the "Basic Models" module of SPM), thereby effecting a random effects model, allowing inference to the general population.

1.3.7 Localization of activations

The stereotactic coordinates of the pixels of the local maximum significant activation were determined within areas of significant relative activity change associated with the tasks. The anatomical localization of these local maxima was assessed with reference to the standard stereotactic atlas (Talairach and Tournoux, 1988), and validation of this method of localization was obtained by superimposition of the SPM-maps on the group mean MR image calculated after each individual's MR image had been stereotactically transformed into the same standard stereotactic space (Friston et al., 1995a).

1.4 Results

1.4.1 Neural activations

Testing for an overall effect of visual search in geometric figures relative to geometric shape recognition revealed a mostly symmetric occipito-parieto-frontal pattern of activations. Bilateral effects ($p_c < 0.05$, corrected) were found in vermis and lateral cerebellum, lateral occipital cortex, posterior parietal cortex, ventral premotor cortex, and the anterior cingulate cortex. Activations specific to the left hemisphere were found in the fusiform and lingual gyri whereas an activation in the anterior insula was confined to the right hemisphere.

Next, we assessed the main effect of *task*. We contrasted the Embedded Figures Task with the control task by calculating C1 + C2 > C3 + C4, masked inclusively by C3 + C4 > baseline. The analysis was conducted in this fashion in order to ensure that activations associated with the Embedded Figures Task were revealed rather than deactivations associated with the control task. The results showed increased neural activity along the left intraparietal sulcus (superior and inferior parietal cortex) and in the left inferior frontal gyrus (Table 1B, Figure 3). The reverse comparison, also masked inclusively, (i.e. C3 + C4 > C1 + C2 masked by C1 + C2 > baseline) did not reveal any significant activations associated with the control task relative to the Embedded Figures Task.

With regard to Factor 2 (*display orientation*), no significant activations were found, neither when contrasting horizontal with vertical presentation of the stimuli nor for the reverse contrast. In the same fashion as for the main effect of task, these comparisons were masked in order to exclude effects due to deactivations relative to the high-level baseline.

Finally, our analysis found no significant interaction between the factors *task* (Embedded Figures Task, control task) and *display orientation* (horizontal, vertical).

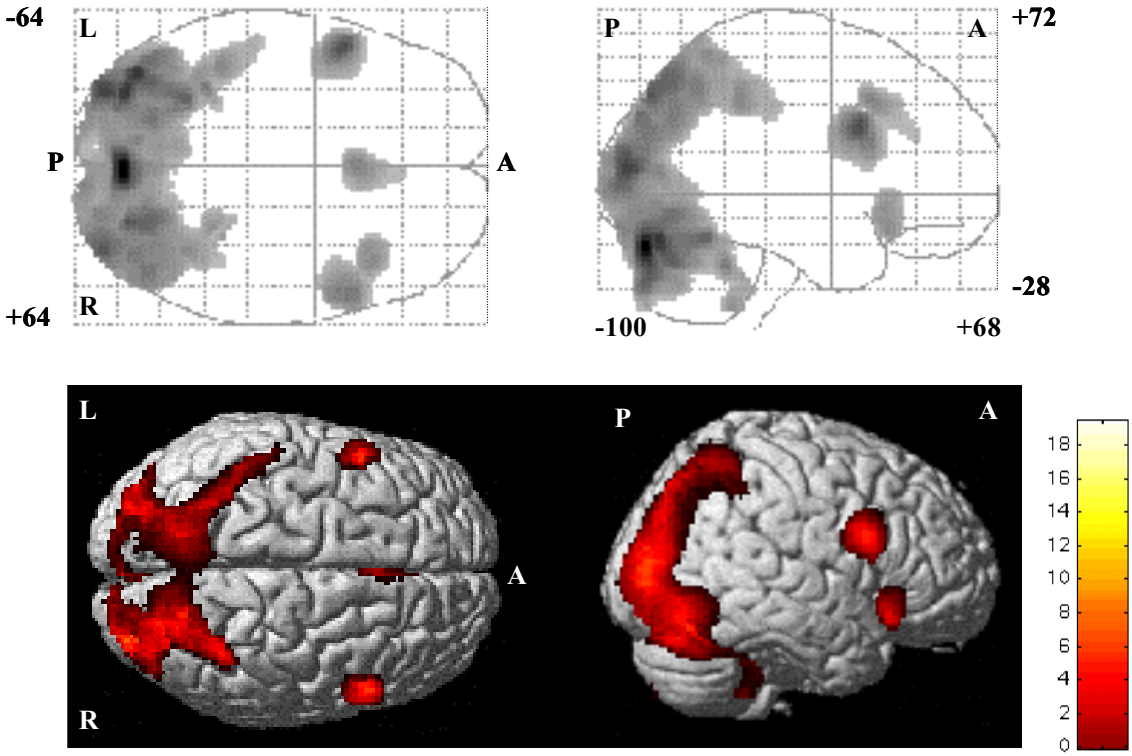

Figure 2: Relative increases in BOLD signal (for the 16 subjects) associated with all four experimental conditions of visual search in geometric structures, i.e. the Embedded Figures Task (EFT) and the control task (CT) using horizontal and vertical stimulus displays, relative to the high-level baseline (geometric shape recognition) (see Methods). Areas of significant relative increase in BOLD signal ($pc < 0.05$, corrected for multiple comparisons) are shown as through-projections onto representations of standard stereotactic space (upper row) and superimposed on a surface rendered representative brain provided by SPM (lower row) to detail the underlying anatomy. The exact coordinates of the local maxima within the areas of activation and their t statistics are given in Table 1 a. R = right, L = left, A = anterior, P = posterior. The numbers on the axes refer to coordinates of standard stereotactic space. The color bar indicates the t-values of the activations.

Next, we assessed the main effect of *task*. We contrasted the EFT with the CT by calculating C1 + C2 > C3 + C4, masked inclusively by C3 + C4 > baseline. The analysis was conducted in this fashion in order to ensure that activations associated with the EFT were revealed rather than deactivations associated with the CT. The results showed increased neural activity along the left intraparietal sulcus (superior and inferior parietal cortex) and the posterior aspect of the left inferior frontal gyrus (Table 3, Figure 4 & Figure 5). The reverse comparison, also masked inclusively, (i.e. C3 + C4 > C1 + C2 masked by C1 + C2 > baseline) did not reveal any significant activations associated with the CT relative to the EFT.

Table 1
Relative increases in brain activity during performance of the Embedded Figures Task and the Control Task.

Region	Side	x	y	z	T_{max}	k	p_c-value
A. Visual search vs. baseline: ¼ (EFT_h + CT_h + EFT_v + CT_v) > BL							
vermis + lateral cerebellum	L/R	2	-80	-24	19.34		
lateral inferior occipital cortex	L	-40	-74	-20	14.40		
	R	46	-70	-18	9.27		
lateral superior occipital cortex	L	-32	-86	12	13.40		
	R	36	-88	18	11.70	18976	0.0001
superior posterior parietal cortex	L	-26	-82	36	9.92		
	L	-20	-68	56	9.55		
	R	24	-78	44	11.57		
fusiform gyrus	L	-28	-54	-20	10.73		
lingual gyrus	L	-20	-68	-10	8.89		
ventral premotor cortex (inferior +	L	-52	12	30	12.50	664	0.001
middle frontal gyrus)	R	56	14	24	8.79	704	0.0001
anterior cingulate gyrus	L/R	-2	16	42	8.07	376	0.012
right anterior insula	R	40	24	-16	7.42	395	0.01
B. Embedded Figures Task: EFT_h + EFT_v > CT_h + CT_v							
ventral premotor cortex (inferior frontal gyrus)	L	-42	10	24	6.77	309	0.022
posterior aspect of intraparietal sulcus	L	-24	-58	54	5.15	279	0.032
anterior aspect of intraparietal sulcus	L	-36	-38	40	5.01		

C

Coordinates are in standard stereotactic space and refer to local maxima of significant clusters of activated voxels. These maxima were indicated by the locally highest T-value (Tmax) within an area of significant activation (p_c-value = corrected p-value) associated with the described contrasts. k is the number of supra-threshold voxels (each at $p < 0.001$, uncorrected) that together constituted the area of significant activation. x is the distance in millimeters to the right (+) or left (-) of the midsagittal line; y is the distance anterior (+) or posterior (-) to the vertical plane through the anterior commissure; and z is the distance above (+) or below (-) the intercommissural line. Anatomical localization is based on the stereotactic atlas and the group mean MRI image. R = right, L = left. EFT_h = Embedded Figures Task, horizontal stimulus orientation; EFT_v = Embedded Figures Task, vertical stimulus orientation; CT_h = control task, horizontal stimulus orientation; CT_v = control task, vertical stimulus orientation.

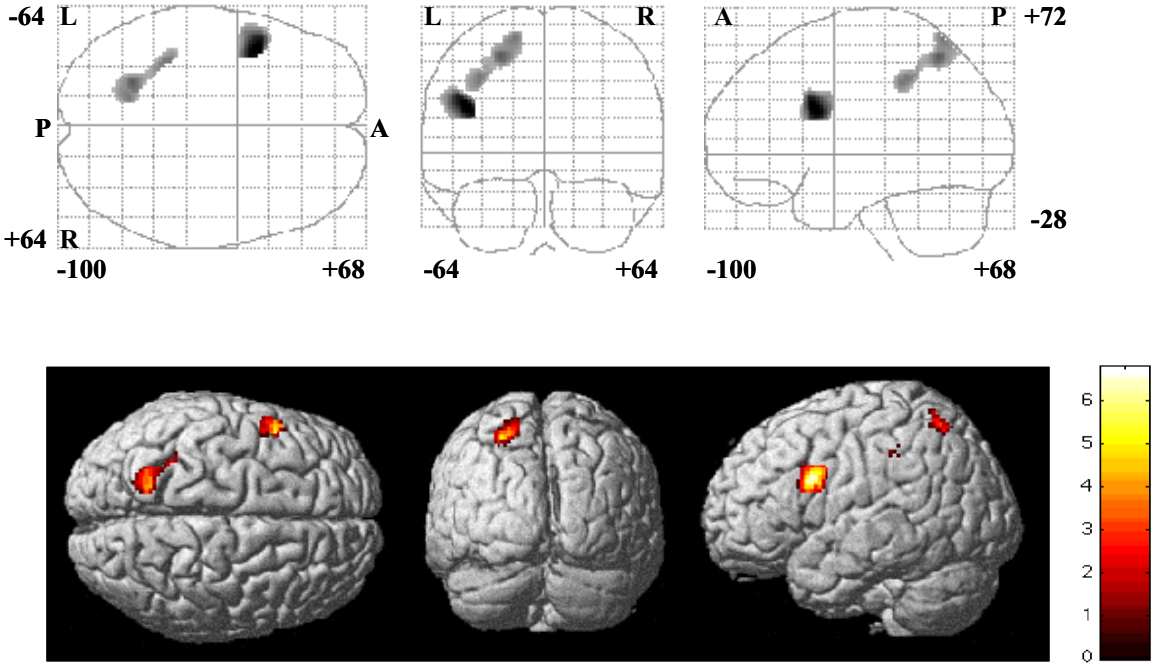

Figure 3. The regions where there is a significant relative BOLD signal increase associated with the Embedded Figures Task relative to the control task ($EFT_h + EFT_v > CT_h + CT_v$). Inclusive masking by $CT_h + CT_v >$ baseline ensures that deactivations relative to baseline are excluded. The exact co-ordinates of the local maxima within the areas of activation and their respective t statistics are given in Table 1 b. Areas of significant relative BOLD signal increases ($p_c < 0.05$, corrected) are shown as through-projections onto representations of standard stereotactic space (for further details see Methods) and superimposed on a surface rendered template brain provided by SPM to detail the underlying anatomy. L = left, R = right, A = anterior, P = posterior. The color bar indicates the t-values of the activations.

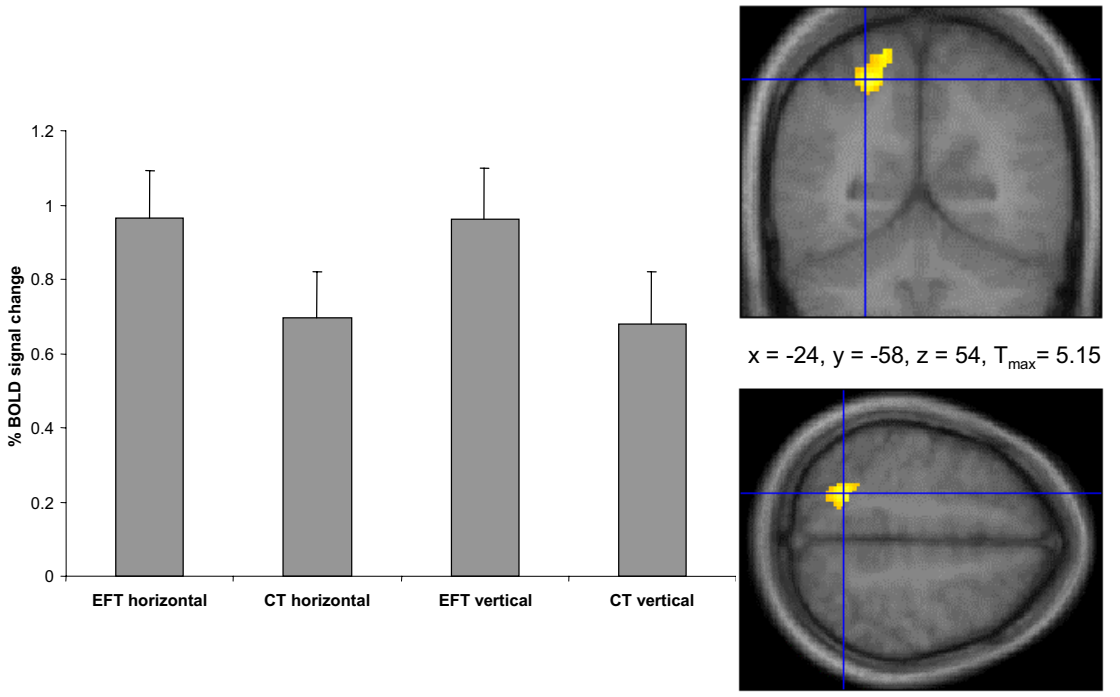

Figure 4. The BOLD signal changes (in percent) per condition are displayed for the local maximum of the maximally significant relative BOLD signal increase within the intraparietal sulcus (x = -24, y = -58, z = 54; see also Table 1 b). The local maximum is shown superimposed onto horizontal and coronal views from the group mean structural magnetic resonance image derived from the subjects studied.

With regard to Factor 2 (*display orientation*), no significant differential activations were found, neither when contrasting horizontal with vertical presentation of the stimuli nor for the reverse contrast. In the same fashion as for the main effect of task, these comparisons were masked in order to exclude effects due to deactivations relative to the high-level baseline.

Finally, our analysis found no significant interaction between the factors *task* (EFT, CT) and *display orientation* (horizontal, vertical).

1.4.2 Behavioural results

Analysis of the behavioral data obtained during scanning revealed that subjects performed the Embedded Figures Task more slowly (2130 ms ± 74 ms; mean ± standard error) and made more errors (14.5 % ± 2.5 %) than during the control task (1569 ms ± 64 ms; 4.1 % ± 1.5 %) (error rates: $F = 31.65$; $df = 1, 15$; $p < 0.001$; reaction times: $F = 46.09$; $df = 1, 15$; $p < 0.001$. Subjects performed the Embedded Figures Task equally well irrespective of display orientation (horizontal: 2129 ms ± 77 ms; 15 % ± 2.6 %; vertical 2132 ms ± 79 ms; 14 % ± 3.1 %). The same was true for the control task (horizontal: 1592 ms ± 66 ms, 3.7% ± 1.6 %; vertical 1546 ms ± 71 ms, 4.6 % ± 1.8 %). Thus, there was no interaction of the factors *task* and *display orientation* (error rates: $F = 2.33$; $df = 1, 15$; $p = 0.148$; reaction times: $F = 0.70$; $df = 1, 15$; $p = 0.415$). A main effect of display orientation did not exist either (error rates: $F < 0.001$; $df = 1, 15$; $p > 0.999$; reaction times: $F = 1.96$; $df = 1, 15$; $p = 0.182$).

Eye movement data were obtained during scanning from all subjects. However, due to calibration problems with the infrared eye measurement device, only data from 8 subjects could be analyzed further. The data were analyzed for total scan path length and the overall time that subjects kept their gaze in the proximity of the stimuli. Analysis of the scan path length data revealed that there were no significant

differences between the Embedded Figures Task (0.270 ± 0.071 pixel/ms [mean scan path ± standard deviation of subjects' means]) and the control task (0.247 ± 0.071; $F = 3.27$, $df = 1, 28$; $p = 0.081$). The overall differences in neural activity between the two tasks thus cannot be ascribed to differential eye movements. While no significant interaction between task and stimuli orientation was found either ($F = 0.11$; $df = 1, 28$; $p = 0.745$), there was a significant main effect of stimuli orientation on the scan path length because of the asymmetrical screen distances between horizontally (0.319 ± 0.039) and vertically (0.199 ± 0.035) arranged stimuli (see Methods; $F = 88.04$; $df = 1, 28$; $p < 0.001$). When these asymmetries were corrected for by restricting the scan path analysis to the vicinity of the stimuli, however, the differences between horizontal (0.222 ± 0.025) and vertical (0.217 ± 0.037) stimulus arrangements became insignificant ($F = 0.19$; $df = 1, 28$; $p = 0.669$).

The similarity of eye movements during the Embedded Figures Task and the control task was corroborated by the analysis of the mean time per block that subjects kept their gaze in the proximity of the stimuli (Embedded Figures Task: 14530 ± 2935 ms, control task: 14346 ± 2906 ms; $F = 0.08$; $df = 1, 56$; $p = 0.775$). While no significant interaction could be found between task and stimulus location ($F = 0.18$; $df = 3, 56$; $p = 0.911$), a main effect of stimulus location (right: 13306 ± 1582; left: 12994 ± 1719; top: 16971 ± 3203; bottom 14480 ± 3022; $F = 7.93$; $df = 3, 56$; $p < 0.001$) was observed. Bonferroni-corrected post-hoc t-tests revealed that subjects spent significantly more time looking at stimuli situated in the upper half of the screen than looking at stimuli in either right, left, or bottom positions ($p < 0.049$). None of the comparisons between right, left, or bottom positions, on the contrary, pointed to significant differences ($p > 0.643$).

1.5 Discussion

This fMRI study shows for the first time which brain regions are involved specifically in the local search aspects of the Embedded Figures Task: namely, left inferior and superior parietal cortex and left ventral premotor cortex. This result does not contradict the finding (Ring et al., 1999) that performance on the task *as a whole* implicates a wide variety of brain regions concerned, for example, with sensory registration of the stimuli, shape analysis, perceptual judgment and decision, and final motor response. Rather, our concern was to isolate what is distinctive about the Embedded Figure Task over and above the components involved in many different tasks concerned with the processing of visual form. In this sense, our findings are complementary to the elucidation by Ring et al. (Ring et al., 1999) of the entire circuit involved in task performance (compared with looking at a blank screen).

It is nonetheless notable that the activations we find to be distinctively implicated in local search as exemplified by the Embedded Figures Task are a proper subset of those reported by Ring et al. (Ring et al., 1999). The coordinates we report (-24, -58, 54) in superior parietal cortex are encouragingly close to those seen in the study of Ring et al. (-15 to –37, -37 to –58, 54) (Ring et al., 1999). Similarly, the coordinates we report in inferior parietal cortex (-36, -38, 40) are very close to the inferior parietal cortex (supramarginal gyrus) activations of Ring et al. (-43, -40, 37). Likewise, the coordinates we report in the left inferior frontal gyrus (-42, 10, 24) are very similar to those reported by Ring et al. (-31, 7, 32; Ring et al., 1999). These differential neural activations associated with the Embedded Figures Task cannot be ascribed to differential eye movements between the Embedded Figures Task conditions and the control task conditions since (i) there were no relevant differential eye movements, (ii) the activations observed are unilateral, and (iii) there was no significant activation of the frontal eye fields.

Comparing horizontal versus vertical arrangements of the stimuli, no significant differences in activations were found in the fMRI data. This absent main effect of display orientation was mirrored behaviorally by the lack of any significant differences in reaction times and error rates. This finding is probably due to the fact that explicit analysis of display orientation is not demanded in either the Embedded Figures Task or the control task; to attend to orientation (over and above merely locating the stimuli) would not aid in solving either task. Furthermore, in our blocked design, subjects already knew where the stimuli would appear on any given trial. That no significant interaction was found between *task* and *display orientation*, indicates that the contrast between local search for a hidden figure and the easier visual search task is unaffected by the spatial layout of the stimuli. Once the stimulus target and the complex figure have been located, local search for that target in the more complex figure is independent of display orientation.

Previous work on related tasks has associated visual search (spatial attentional shifts) with activation of superior parietal cortex (Corbetta et al., 1995; Fink et al., 2000). Activation of left inferior parietal cortex has been associated with object-based visual attention (Fink et al., 1997a) and with locally directed visual attention in tasks involving hierarchically organized visual stimuli: that is, stimuli with both a local and a global organization (Fink et al., 1996; Fink et al., 1997b; Weber et al., 2000). This overall pattern of results increases the prima facie validity of our claim that activation of left superior and inferior parietal cortex during performance of the Embedded Figures Task is specifically related to visual search for local targets (Corbetta and Shulman, 1998). Nonetheless, many versions of the Embedded Figures Task are probably much harder than more typical local / global processing tasks (Miller and Navon, 2002) due to the fact that the target figure is indeed *hidden* in the more complex form. It is this latter characteristic that makes the Embedded Figures Task

such a distinctive and useful clinical test. Other visual tasks involving either serial or parallel (pop-out) search do not typically 'hide' the targets within a global pattern (see chapter 11 of Palmer, (Palmer, 1999).

Concerning the association between aphasia and impaired performance on the Embedded Figures Task (Teuber and Weinstein, 1956), the region that we find activated in inferior parietal cortex is quite close to the posterior language areas of the left hemisphere (Benson, 1979). Many central reading and writing disorders are also consequent upon lesion of the left supramarginal gyrus (Heilman and Valenstein, 1993). Likewise, the region of the left inferior frontal gyrus that we find activated is part of the anterior language area (Amunts et al. 1999). Although large left hemisphere lesions may well provoke both aphasia and impairment on the Embedded Figures Task (Corkin, 1979), it seems unlikely that the latter impairment is dependent primarily on the sheer extent of the cerebral pathology, contrary to the claims of Teuber and Weinstein (Teuber and Weinstein, 1956) and Cobrinik (Cobrinik, 1959). Rather, our results show that two comparatively small regions are associated specifically with local search on the Embedded Figures Task. This finding is consistent with the claim of Russo and Vignolo (Russo and Vignolo, 1967) and Orgass et al. (Orgass et al., 1972) that both large and small lesions can give rise to impairments on this task.

Although most studies of subjects with autism or Asperger's syndrome have found superior local search (Jollife and Baron-Cohen, 1997; Happé, 1999) and inferior global processing (Rinehart et al., 2000), controversy remains concerning the precise characterization of these patterns of performance and their generality across the autistic spectrum (Ropar and Mitchell, 2001). For example, Plaisted, Swettenham and Rees (Plaisted et al., 1999) confirmed that autistic children show local

precedence in a divided attention task, but found global precedence in a selective attention task. Mottron, Burack, Stander and Robaey (Mottron et al., 1999) found, contrary to many reports, that their sample of high-functioning children and adolescents with autism showed relatively intact global processing. But the overall consensus of work on both autism (Shah and Frith, 1983) and on Williams syndrome (Bihrle et al., 1989) is that processing style in both conditions favors local (detail-focus) processing at the expense of the global configuration which does not automatically capture their attention. The relationship of this global deficit (or processing de-emphasis) to malfunction of right occipito-temporal cortex deserves sustained investigation in both acquired (Doyon and Milner, 1991) and developmental disorders (Jambaque et al., 1998). We know that autistic individuals find hidden figures easily, but the question is why. In future studies, it may be pertinent to contrast hierarchically structured displays in which target figures can be easily hidden with unstructured displays in which target figures are not so easily hidden.

We do not discuss these issues further here as the nature of the deficit in autism or Williams syndrome is not the main thrust of this paper, although we hope that our findings will inform future research on local / global processing in these conditions (Happé and Frith, 1996). Nonetheless, it is important to understand the neural mechanisms underlying visual search for hidden figures in healthy volunteers before investigating this issue in pathological conditions. More directly, we suggest that clinical neuropsychological studies of the Embedded Figures Task (and related tests) may usefully adopt a variant of the subtraction technique that is employed here and in many other functional imaging studies. In particular, we propose that control tasks similar to the one deployed in the current experiment are pertinent to studies that aim to discover the lesion sites associated with impairments of local search; the ability to

perform within normal limits on such control tasks would help to ensure that any impairment on tasks that involve the detection of hidden (embedded) figures was indeed specific to the local search aspect of such tasks.

2. Context-dependent interactions of left posterior inferior frontal gyrus in a local visual search task unrelated to language

This chapter contains the following publication:

Manjaly ZM, Marshall JC, Stephan KE, Gurd JM, Zilles K & Fink GR (2005) Context-dependent interactions of left posterior inferior frontal gyrus in a local visual search task unrelated to language. Cognitive Neuropsychology 22: 292-305.

2.1 Summary

The Embedded Figures Task (EFT) involves search for a target hidden in a complex geometric pattern. Even though the EFT is designed to probe local visual search functions, not language-related processes, neuropsychological studies have demonstrated a strong association between aphasia and impairment on this task. A potential explanation for this relationship was offered by a recent functional MRI study (Manjaly et al., NeuroImage 19:674-683, 2003) which demonstrated that a part of the left posterior inferior frontal gyrus (pIFG), overlapping with Broca's region, is crucially involved in the execution of the EFT. This result suggested that pIFG, an area strongly associated with language-related functions, is also part of a network subserving cognitive functions unrelated to language. In this study, we tested this conjecture by analyzing the data of Manjaly et al. for context-dependent functional interactions of the pIFG during execution of the EFT. The results showed that during EFT, compared to a similar visual matching task with minimal local search components, pIFG changed its interactions with areas commonly involved in visuospatial processing: Increased contributions to neural activity in left posterior parietal cortex, cerebellar vermis, and extrastriate areas bilaterally, as well as decreased contributions to bilateral temporo-parietal cortex, posterior cingulate cortex, and left dorsal premotor cortex were found. These findings demonstrate that

left pIFG can be involved in non-language processes. More generally, however, they provide a concrete example of the notion that there is no general one-to-one mapping between cognitive functions and the activations of individual areas. Instead, it is the spatiotemporal pattern of functional interactions between areas that is linked to a particular cognitive context.

2.2 Introduction

In the Embedded Figures Task (EFT), initially developed by Gottschaldt (1926, 1929), participants are presented with two geometric figures on each trial: a complex and a simple one. The objective is to decide whether the simpler figure is "embedded" in the complex one (i.e. is a subpart thereof). The task thus requires one to search the complex figure for intrinsic patterns that could match the simpler figure, i.e. the subjects' visual search is guided and constrained by the simple figure and the local characteristics of the complex figure. In neuropsychological studies, the EFT has been used to investigate characteristics of local perception and visual search, both in normal subjects and various patient groups. One intriguing finding from these investigations is that both autistic subjects and unaffected relatives often show superior EFT performance as compared to normal controls (Baron-Cohen & Hammer 1997; Happe 1999; Shah & Frith 1983). These results have been interpreted as evidence for the hypothesis of "weak central coherence" in autistic patients, i.e. the tendency to bias visual information processing towards the local rather than the global level (Happe 1999).

While the application of the EFT in autism research has created long-lasting interest and has led to numerous applications, including functional imaging studies (Ring et al. 2000), it is less well known that some curious findings had been obtained when testing patients with acquired brain damage on the EFT. An interesting

relationship between left-hemisphere lesions and EFT performance was first revealed in a clinical study by Teuber & Weinstein (1956): patients suffering from aphasia unexpectedly showed greater impairment on the EFT than patients with other neuropsychological deficits. Subsequent studies replicated this finding, demonstrating additionally that (i) this association did not depend on the extent of brain damage as such, and (ii) that the impairment was not due to failure to understand the task instructions (Orgass et al. 1972; Russo & Vignolo 1967). These results were puzzling since the EFT is not obviously related to language processing, but rather to local visuospatial processing. A convincing explanation for the association between aphasia and impaired EFT performance has been lacking for a long time, although the well-known left-hemisphere advantage for local processing (Robertson et al. 1988; Fink et al. 1996, 1997; Marshall & Fink 2001) may at least in part contribute to this association.

Recently, a functional magnetic resonance imaging (fMRI) study which contrasted the EFT with a similar but simpler visual matching task that minimized the local search aspects identified the cortex around the left intraprietal sulcus (IPS) and, more interestingly, a region extending from the ventral part of the precentral gyrus across the precentral sulcus into the posterior part of the inferior frontal gyrus (pIFG) as areas crucially involved in the local search aspects of the EFT (Manjaly et al. 2003). The spatial extent of the activation in the left pIFG overlapped with the dorsal part of Broca's region, i.e. areas 44 and 45, as defined by observer-independent cytoarchitectonic techniques (Amunts et al. 1999). Its local maximum (x = -42, y = 10, z = 24) possessed coordinates in good correspondence to those provided by previous fMRI studies on various aspects of language processing (e.g. Poldrack et al. 1999; Stephan et al. 2003). There is overwhelming evidence, both from lesion and functional imaging studies, that left pIFG is associated with various aspects of

language function. Therefore, the strong activation of this region when subjects undertake the EFT provides an explanation for the association of aphasia and impaired EFT performance.

It remains to be explained, however, why a region like the left pIFG that is normally found to be involved in language processing, should play any role at all during a local visual search task like the EFT which does not seem to require any language-related processing. One possible explanation is that pIFG is involved in the EFT simply because the EFT contains a language-related component that we and previous researchers had not been aware of (the “hidden language component hypothesis”). But neither the simple nor the complex figures typically used in the EFT are easily namable. An alternative hypothesis is that left pIFG participates in different cortical networks subserving different cognitive functions, depending on the context of the overall task. This idea of “neural context”, i.e. the context-dependent binding of a given area into different networks has previously been formulated by McIntosh (2000) who suggests that “a particular region in isolation may not act as a reliable index for a particular cognitive function. Instead, the neural context in which an area is active may define the cognitive function. Neural context emphasizes that the particular spatiotemporal pattern of neural interactions may hold the key to bridge between brain and mind." From this perspective, understanding the potential range of function of an area requires us to understand its *context-dependent interactions with other areas*. This view represents a change from the investigation of functional specialization, as it has been conceived in the large majority of neuropsychological and functional imaging studies to date, towards the characterization of *functional integration* in the brain (Friston 1998).

In the present study, we have applied this concept to the fMRI study by Manjaly et al. (2003) and have re-analyzed the data, using a simple model of effective connectivity (Friston 1994). Specifically, we have used "psychophysiological interactions" (PPI; Friston et al. 1997) to investigate the context-dependent functional contributions of left pIFG to brain responses elsewhere. If the "hidden language component hypothesis" is correct and pIFG function is indeed largely or entirely dedicated to language or language-like tasks, its pattern of functional interactions during the EFT, as compared to the control task, should include other language-related areas, e.g. in the left temporal lobe. On the other hand, if the hypothesis of "neural context" is correct, we would expect that comparing the functional interactions of left pIFG during the two different visuospatial search tasks of our experiment should reveal changes in pIFG connectivity only with areas associated with visuospatial rather than language processing, e.g. posterior parietal, extrastriate, and dorsal premotor regions.

2.3 Methods

Details of the experimental design, data acquisition, and data analysis have been published previously (Manjaly et. al. 2003). Here, we briefly summarize the methods and then focus on the analysis of effective connectivity, using psycho–physiological interactions (PPIs; see Friston et al. 1997).

2.3.1 Subjects

Sixteen healthy, right-handed male volunteers (aged 20 to 36 years; mean age 24.3 years ± standard deviation 4.3 years) with no history of neurological or psychiatric illness were studied. The study was approved by the ethics committee of the University Hospital Aachen. Informed written consent was obtained prior to participation.

2.3.2 Stimuli and experimental design

The initial aim of this experiment was to localize brain activations that were specific to the local search aspects of the EFT. Therefore, we compared the EFT to another closely related but easier visual search task (referred to as "control task") that operated on similar visual stimuli and also engaged visual search, shape analysis, visual matching, decisions about geometrical configurations, and motor responses, but which minimized local visual search processes, as the stimuli were disambiguated, i.e. a figure within the complex figure was highlighted (see below). To investigate whether the spatial arrangement of the stimuli had an influence of how the tasks were performed, we used horizontally and vertically arranged pairs of stimuli equally often. We thus dealt with a 2x2 factorial design with *task* (EFT vs. control task) and *stimulus orientation* (horizontal vs. vertical) as experimental factors.

All stimuli were produced using a PC graphics program (Corel Draw 9.0, Corel Corp). 32 geometrical figures consisting of 12 lines and of comparable complexity were created. Each of these complex figures was presented eight times throughout the course of the experiment, i.e. twice in each of the four conditions. In all conditions, each complex figure was accompanied by a simple target figure. These target figures were either embedded into the simultaneously presented complex figures (50% of trials) or were not part of any of the complex figures shown on any trial (50% of trials). Each correct target figure was only shown once throughout the entire experiment to minimize priming effects. Since the incorrect target figures were not embedded in any of the complex figures used in the experiment, they could safely be used twice, i.e. once in each task. Fig. 1 shows examples of the figures used as stimuli during the EFT and the control task, and also summarizes the factorial design of the experiment. For the EFT, subjects were instructed to indicate via right hand button press whether or not the target was embedded in the complex

figure. During the control task, subjects were presented with the same stimuli which were, however, disambiguated: i.e. a simple figure within the complex figure was highlighted. For this task, subjects were instructed to indicate via right hand button presses whether or not the target figure matched the simple figure highlighted within the complex figure. The conditions were blocked with each block containing 8 trials (each with a stimulus on time of 3 seconds) and lasting 32 seconds in total. Between conditions, a “baseline” (lasting 24 sec) was implemented, in which subjects viewed squares or triangles presented centrally and had to indicate via right hand button presses whether or not the figure presented was a square. Before the beginning of each block, instructions of the subsequent task were given for 4 seconds, informing the subject which task to perform and whether the stimuli were arranged horizontally or vertically. The condition sequence was pseudorandomized and counterbalanced across subjects. In order to allow for short break periods, the experiment was split into 4 consecutive sessions. Each session consisted of 8 task blocks alternating with 8 baseline blocks. Thus, the experiment included 32 task blocks (16 EFT blocks, 16 control task blocks) and 32 baseline blocks altogether.

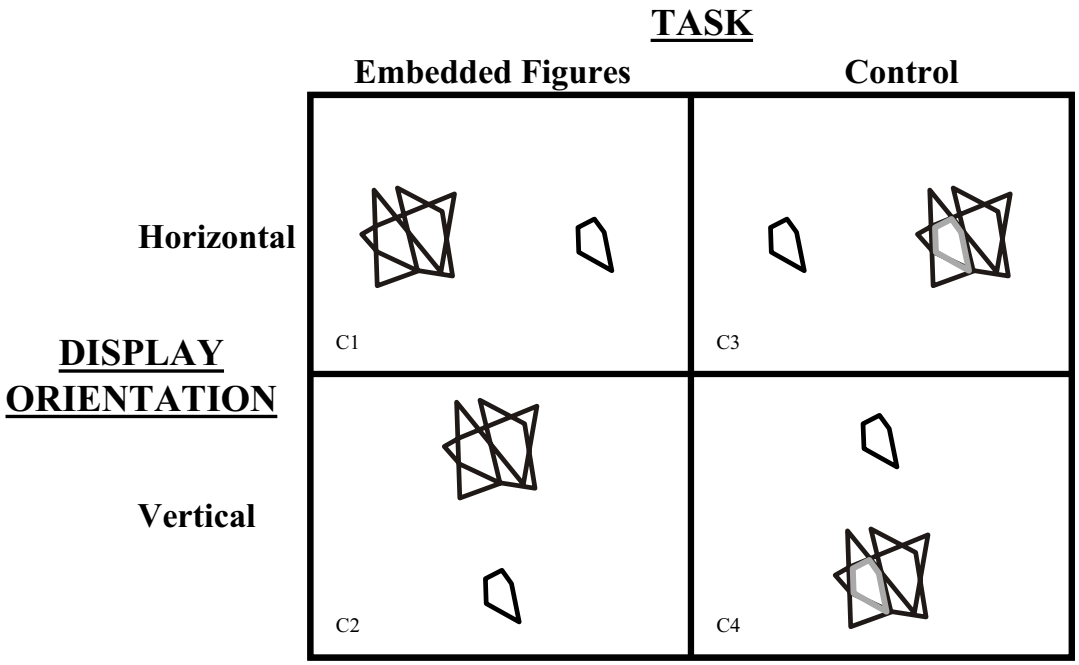

Figure 1. Stimuli and study design. Examples of the stimuli used for the Embedded Figures Task and the control task. Stimuli were displayed either horizontally or vertically. In the EFT subjects judged whether the target figure was or was not embedded in the more complex figure. In the control task subjects judged whether the target figure did or did not match the highlighted figure (indicated in grey) within the complex figure.

Behaviorally, reaction times and error rates were recorded as measures of task difficulty and task performance. Additionally, as the tasks were undertaken in free vision, we recorded eye movements in all subjects during the MR measurements to assess whether differential eye movements occurred in the Embedded Figures Task and control conditions. An fMRI-compatible infrared video-based eye-tracking device (ASL 504; Applied Science Laboratories, Bedford, MA, USA) was used for this purpose. Details of the analysis of the behavioral data can be found in our previous article (Manjaly et al. 2003).

2.3.3 MRI data acquisition

Magnetic resonance imaging was performed on a Magnetom Vision 1.5 Tesla scanner (Siemens Medical Systems GmbH, Erlangen, Germany) using a standard head coil. For each subject, a high-resolution, T1-weighted anatomical image was obtained using a MP-RAGE sequence. Functional images were obtained by means

of an Echo Planar Imaging (EPI) sequence with the following parameters: gradient echo EPI; TE = 66 ms; TR = 4s; FOV = 200 x 200 mm; flip angle = 90°; matrix size = 64 x 64; pixel size = 3.125 x 3.125 mm; slice thickness = 4.0 mm; inter-slice gap = 0.4 mm; 30 slices. At the beginning of each session, 4 dummy scans were obtained to allow the MR signal to reach a steady state.

2.3.4 fMRI analysis

Spatial pre-processing and statistical analysis of fMRI data were performed using MATLAB 5.3 (The Mathworks Inc., Natick, MA, USA) and SPM99 software (Statistical Parametric Mapping; Wellcome Department of Imaging Neuroscience, London, UK; http://www.fil.ion.ucl.ac.uk/spm). The first four dummy images of each session were discarded. The remaining 128 volume images of each time-series were realigned to correct for head movements during scanning. Models of effective connectivity which are based on variants of regression analysis assume that data points from different time series have been acquired simultaneously. Since this is not the case in multi-slice acquisition fMRI, we corrected for differences in the acquisition times of the 30 slices by linear interpolation in time (slice timing), using the middle slice as a reference point. All functional images were then co-registered to the 3D anatomical image and transformed into the Montreal Neurological Institute (MNI) stereotactic space which is based on the Talairach system (Talairach and Tournoux, 1988). Resampling after this non-linear warping procedure (Friston et al., 1995a; Ashburner & Friston 1999) led to a resulting pixel size of 2 x 2 x 2 mm. Transformed functional images were smoothed with a Gaussian kernel of 10 mm full width half maximum (FWHM) for the group analysis to meet the statistical requirements of the General Linear Model and to compensate for normal variation in individual brain size, shape and sulcal / gyral anatomy.

Following spatial pre-processing, statistical analysis was performed using a General Linear Model in SPM99 (Friston et al. 1995b). Low frequency signal drifts were removed by a high pass filter (cutoff: 0.0075 Hz). Global means were normalized by proportional scaling. Data were analyzed by modeling the different conditions as reference waveforms (i.e. box car functions convolved with a canonical hemodynamic response function). For each subject, the design matrix included regressors for the 5 conditions (i.e. 4 task conditions, one baseline condition) and twelve regressors with realignment parameters (six absolute and six differential parameters describing rotation and translation of the subject's head). Following parameter estimation, effects of interest were tested by applying appropriate linear contrasts, resulting in a t-statistic at each voxel. These t-statistics (transformed to Z-statistics) constitute a subject-specific statistical parametric map (SPM{Z}). The SPM{Z} maps were then interpreted by referring to the probabilistic behavior of Gaussian random fields. In all analyses, areas of activation were identified as significant only if they passed a threshold of $p_c < 0.05$, corrected for multiple comparisons at the cluster level (Friston et al., 1995b; Poline et al. 1997).

For the fMRI data group analysis, the contrast images from the analyses of the individual subjects were analyzed by one sample t-tests. This constituted a random effects model which allows inference to the population from which the sixteen subjects were drawn (Friston et al. 1999).

Details and results of the above analysis have been reported by Manjaly et al. (2003). Its methodological principles are briefly repeated here because the results form the starting point for the analysis of effective connectivity which is the central topic of this article. Specifically, in the present study we used a variant of psycho-physiological interactions (Friston et al. 1997) to determine all brain areas that

received a context-dependent contribution from the posterior part of the left inferior frontal gyrus (pIFG) cortex. First, the analysis described above was repeated for each subject, using the identical design matrix but smoothing the data spatially with a smaller kernel, i.e. 6 mm FWHM, to obtain a higher regional specificity for the left pIFG time series. For each subject, we then determined the local maximum of the left pIFG activation in the EFT vs. control task contrast that was closest to the group maximum in the random effects analysis for this contrast. In order to select voxels in which our model optimally explained the variance of the data, this local pIFG maximum was determined from an F-contrast spanning all effects of interest. Individual time series for the left pIFG were obtained by extracting the first principal component from all voxel time series within a sphere (6 mm radius) centered on the chosen pIFG coordinates. This procedure for extracting characteristic regional time series is widely used in analyses of effective connectivity (compare, for example, Büchel & Friston 1997; Rowe et al. 2002; Stephan et al. 2003). The resulting time series were mean-corrected and high-pass filtered to remove low-frequency signal drifts, but were not manipulated otherwise. After these time series had been chosen, the actual PPI analysis could be prepared. The psycho-physiological pIFG×task interaction term (referred to as “PPI regressor”) was computed as the element-by-element product of the mean-corrected left pIFG time series and a mean-corrected task vector coding for the main effect of task (1 for each scan during the EFT, -1 for each scan during the control task, and 0 elsewhere). Prior to multiplication, this task vector was convolved with a canonical hemodynamic response function (to account for the hemodynamic lag) and mean-corrected. The PPI regressor was mean-corrected and orthogonalized with regard to the main effect of task and the pIFG time series. In addition to the PPI regressor and the pIFG time series per se, the model of effective connectivity included the main effects of task and stimulus orientation, the

baseline condition, and effects of no interest (instruction periods, movement regressors). Altogether, our analysis of effective connectivity was thus specific for context-dependent pIFG influences that occurred over and above any task effects and context-independent pIFG influences (compare Macaluso et al. 2000; Stephan et al. 2003). Brain sites receiving contextual pIFG influences that were stronger during EFT than during the control task were determined by testing for positive slopes of the PPI regressor, i.e. by applying a t-contrast that was 1 for the PPI regressor and 0 elsewhere. Conversely, areas receiving contextual pIFG influences that were weaker during the EFT than during the control task were found by testing for negative slopes of the PPI regressor, i.e. by applying a t-contrast that was –1 for the PPI regressor and 0 elsewhere. Subject-specific contrast images were smoothed spatially (using a Gaussian kernel of 8 mm FWHM; together with the initial 6 mm smoothing, this resulted in an overall smoothness of 10 mm FWHM) and then entered into random effects group analyses. As in the conventional SPM analysis described above, the significance of the results was assessed by correcting for multiple comparisons across the whole brain, using a corrected threshold of $p<0.05$ at the cluster-level (with $p<0.001$ at the voxel-level).

2.4 Results

As reported in Manjaly et al. (2003) in detail, comparing Embedded Figures Task (EFT) vs. the control task (CT) showed significant clusters of activation in the posterior part of the left inferior frontal gyrus (pIFG; local maximum at x = -42, y = 10, z = 24; $t_{max} = 6.77$; $p<0.05$, corrected) and along the left intraparietal sulcus (-24, -58, 54; $t_{max} = 5.15$; $p<0.05$, corrected). Fig. 2 summarizes the results of this previous analysis.

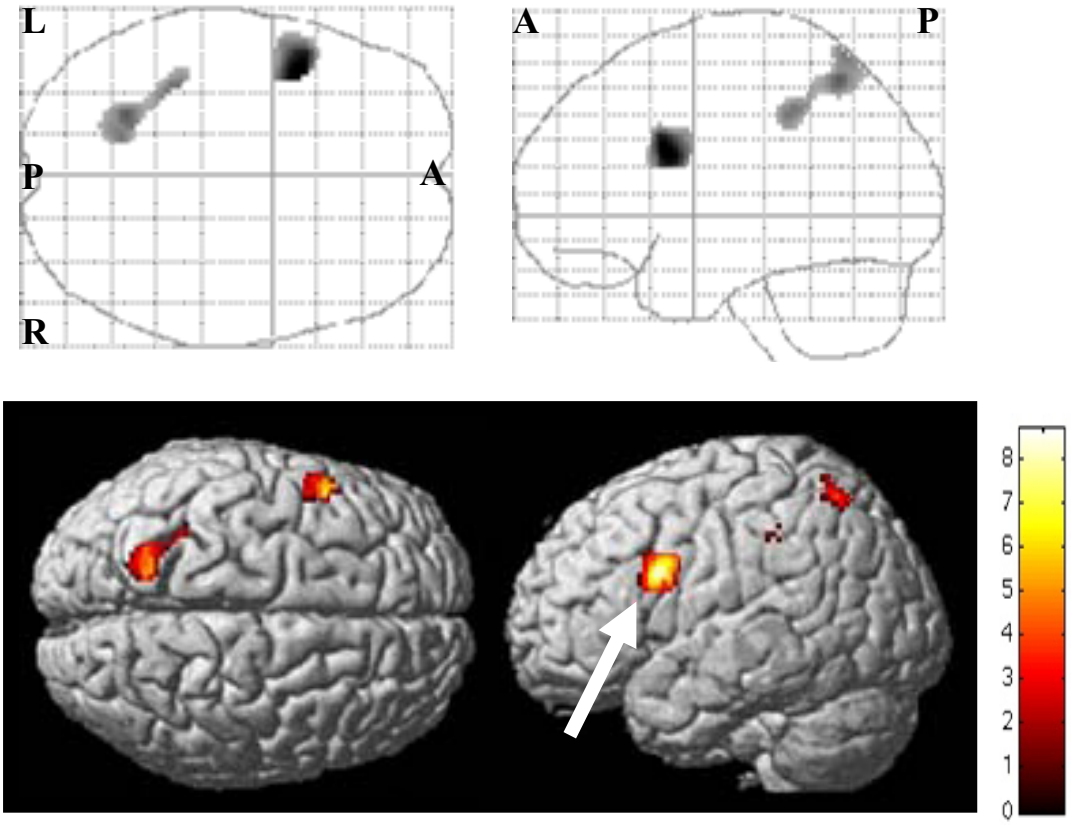

Figure 2. Main effect of task (EFT vs. CT) as reported by Manjaly et al. (2003), random effects analysis (16 subjects). All activations from the EFT vs. CT contrast (masked inclusively by the CT vs. baseline contrast), significant at a cluster-level corrected threshold of p_.05, are shown.Top row: Maximum intensity projections (glass brains). A_anterior, P_posterior, L_left, R_right. Bottom row: Activations overlaid on a rendered template brain. The colour bar indicates t-values. The white arrow points to the activation in the posterior inferior frontal gyrus that represented the starting point for the analysis in this paper.

The local maximum of this activation in the left pIFG served as the starting point for the PPI analysis in this paper. As described in the Methods section, for each subject we determined the local pIFG maximum in the "effects of interest" F-contrast that was closest to the group maximum of the EFT>CT contrast and extracted a characteristic regional time series as the basis for the subject-specific PPI analysis. The contrast images resulting from testing for positive and negative regression slopes of the PPI regressor (i.e. the pIFG×task interaction term), respectively, were then entered into standard random effects group analyses of all sixteen subjects. All results reported below have been corrected for multiple comparisons across the whole brain, using a corrected cluster-level threshold of $p<0.05$ (with $p<0.001$ at the voxel-level).

In the random effects group analysis, areas that showed an *increased* contribution from left pIFG during EFT as compared to CT included the left posterior parietal cortex (local maximum at -18, -62, 58; t_{max} = 6.77; p<0.01; Fig. 3A,B), extrastriate areas bilaterally (left hemisphere: -18, -90, 26; t_{max} = 5.47; p<0.001; right hemisphere: 26, -84, 22; t_{max} = 4.63; p<0.014; Fig. 3A,C), and the cerebellar vermis (2, -64, -50; t_{max} = 4.60; p<0.014; Fig. 3A). In contrast, areas which received a *decreased* contribution from the left pIFG during EFT relative to CT included the temporo-parietal cortex bilaterally (left hemisphere: -50, -56, 20; t_{max} = 6.82; p<0.001; right hemisphere: 46, -56, 30; t_{max} = 5.26; p<0.001; Fig. 4A,B), the posterior cingulate cortex bilaterally (0, -38, 26; t_{max} = 5.38; p<0.007; Fig. 4A), and the left dorsal premotor cortex (-38, 12, 54; t_{max} = 7.02; p<0.001; Fig. 4A).

To complete the characterization of context-dependent functional interactions in our paradigm, we performed analogous PPI analyses for the second area which, in the conventional SPM analysis, had demonstrated significantly higher activity during the EFT relative to the control task, i.e. the left IPS. In this second PPI analysis, the only area that showed an increased contribution from the left IPS during EFT as compared to CT was the right posterior parietal cortex (18, -62, 42; t_{max} = 6.69; p<0.001; Fig. 5A). Similar to the PPI results for the left pIFG, the left temporo-parietal cortex (-58 , -50, 16; t_{max} = 4.57; p<0.001; Fig. 5B) was found to receive a decreased contribution from the left IPS during EFT compared to the control task.

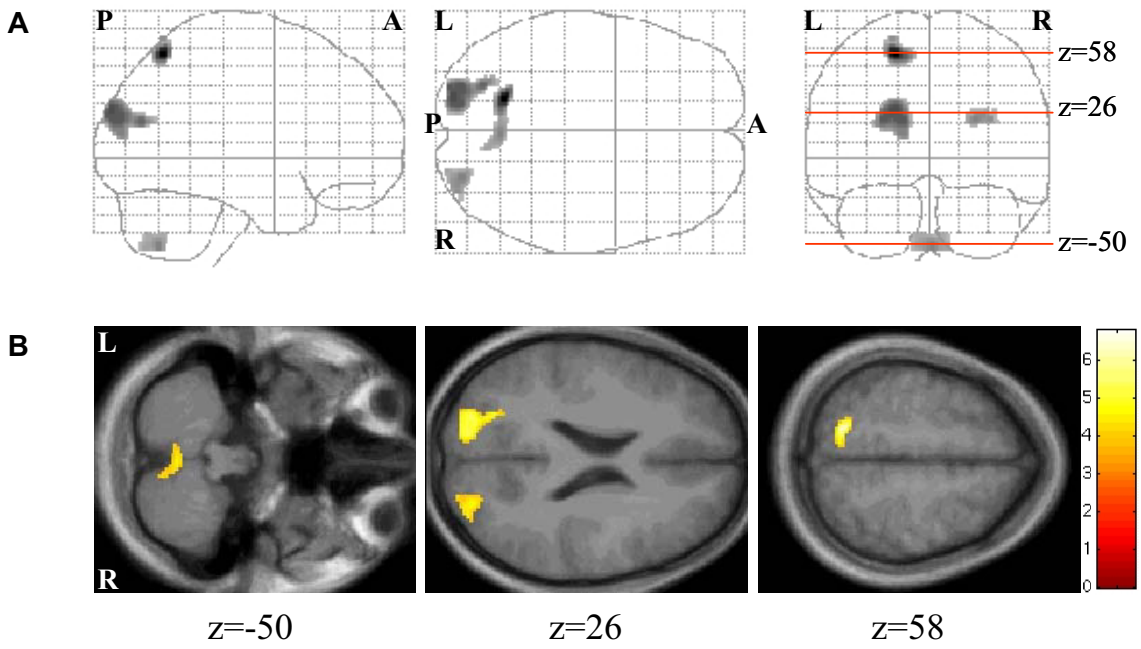

Figure 3. Results of the PPI analysis, random effects analysis (16 subjects). All areas are shown that received an increased influence from left pIFG during EFT relative to CT. Cluster-level threshold of $p<0.05$, corrected for multiple comparisons across the whole brain (voxel-level threshold of $p<0.001$). (A) Maximum intensity projections (glass brains) of the results: sagittal (left), horizontal (middle), and coronal (right) views. Red lines indicate the approximate locations of the sections in Fig. 7B (B) Horizontal sections showing significant increases of left pIFG contribution to the cerebellar vermis (left), extrastriate cortex (middle), and left posterior parietal cortex (right). Activations are overlaid on the averaged normalized structural image of all 16 subjects. z-coordinates denote the horizontal level at which sections were taken from – see Fig. 3A, right panel.

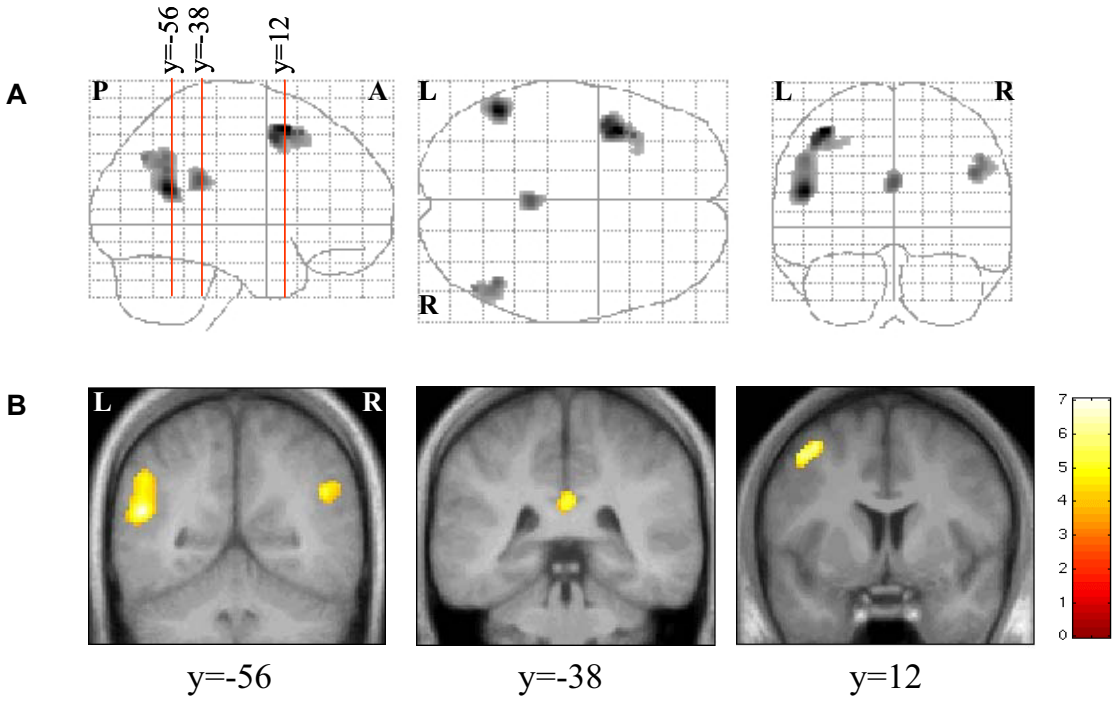

Figure 4. Results of the PPI analysis for left pIFG, random effects analysis (16 subjects). All areas are shown that receive a decreased influence from left pIFG during EFT relative to CT. Conventions and abbreviations as in Fig. 6. (A) Red lines indicate the approximate locations of the sections in Fig. 7B. (B) Coronal sections showing significant decreases of left pIFG contribution to the bilateral temporo-parietal junction (left), posterior cingulate cortex (middle), and left dorsal premotor cortex (right). y-coordinates denote the coronal level at which sections were taken from – see Fig. 4A, left panel.

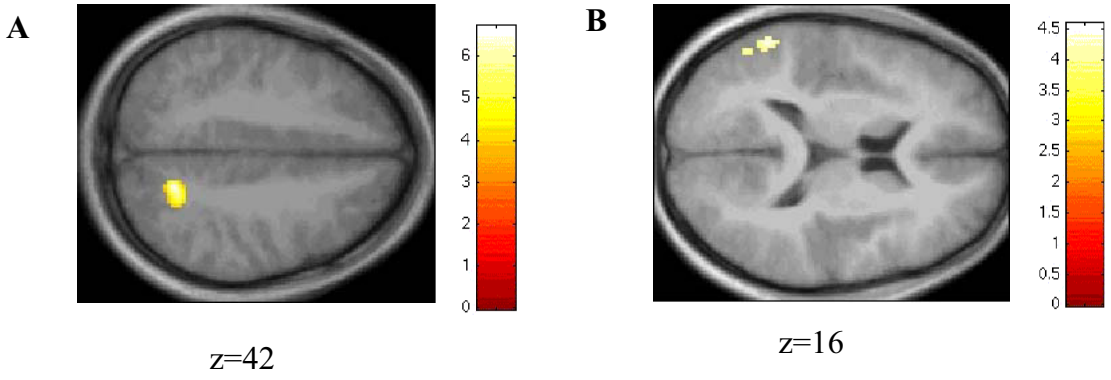

Figure 5. Results of the PPI analysis for left IPS, random effects analysis (16 subjects). As in Figs.6&7, results are shown at a cluster-level threshold of p<0.05, corrected for multiple comparisons across the whole brain (voxel-level threshold of p<0.001). (A) The only area to receive an increased contribution from left IPS during EFT as compared to the CT was the right posterior parietal cortex (18, -62, 42; t_{max} = 6.69; p<0.001). (B) Similar to the PPI results for the left pIFG (compare Fig. 7), the left temporo-parietal cortex (-58 , -50, 16; t_{max} = 4.57; p<0.001) was found to receive a decreased contribution from the left IPS during EFT relative to the CT.

2.5 Discussion

The present study complements and extends the findings by Manjaly et al. (2003) in explaining a repeatedly observed association between aphasia (due to left-hemispheric lesions) and impaired performance on the EFT (Orgass et al. 1972; Russo & Vignolo 1967; Teuber & Weinstein 1956). Manjaly et al. (2003) demonstrated that a region in the left pIFG showed significantly higher activity during the EFT compared with a similar visual matching control task that made only minimal use, however, of local visual search processes. In this study, we re-analyzed the data by Manjaly et al. (2003) and investigated context-dependent functional interactions of the left pIFG to distinguish between two possible explanations why left pIFG, which is usually associated with language processing, might be involved in the execution of the EFT. One hypothesis was that pIFG is activated during the EFT because performing the EFT might involve a "hidden" language-related component that had simply gone unnoticed so far. If this "hidden language component hypothesis" was correct and left pIFG function during the EFT was linked to language processes, we would expect to find significant changes in functional interactions with language-related areas, e.g. in the left temporal lobe, during the EFT as compared to the control task. The alternative hypothesis was based on the idea of "neural context" (McIntosh 2000; McIntosh et al. 2003), i.e. depending on task requirements: left pIFG may be able to participate in different cortical networks and could thus contribute to different cognitive processes. If this hypothesis was correct and left pIFG could also become involved in local visual search processes, we expected that comparing the functional interactions of left pIFG during the two different visuospatial tasks of our experiment should demonstrate significant changes in coupling predominantly with areas typically involved in visuospatial processing.

In order to assess context-dependent functional interactions and decide between the two hypotheses above, we computed psycho-physiological interactions of the left pIFG. Importantly, this method does not determine absolute degrees of coupling, but computes the *difference* in the functional contributions of a source area to voxels elsewhere between two different contexts (Friston et al. 1997). Since we had no strong hypotheses on the type of coupling changes induced by alternating between the two tasks, we determined the entire set of areas that showed a significant difference in coupling with left IFG between the EFT and the control task, regardless of the direction of this difference.

The results of our PPI analyses provided evidence that pIFG function is not exclusively linked to language, but can cooperate with areas that commonly subserve visuospatial functions: during the EFT (relative to the control task), left pIFG increased its contribution to left posterior parietal cortex, bilateral extrastriate cortex, and the cerebellar vermis, and decreased its contribution to left and right temporo-parietal cortex, posterior cingulate cortex, and left dorsal premotor cortex (see Figs. 3, 4). The involvement of all these areas in various aspects of visuospatial processing has been demonstrated by a series of previous imaging studies (e.g. Corbetta et al. 2000; Fink et al. 2000, 2001; Gitelman et al. 2002; Hopfinger et al. 2000; Kim et al. 1999; Yantis et al. 2002). In contrast, to our knowledge, only two of these areas have been implicated in language processing as well: left temporo-parietal cortex activation has previously been observed during the processing of spoken language (Binder et al. 1997), and the left dorsal premotor cortex has been linked to verbal working memory (Herwig et al. 2003). These cognitive processes, however, are highly unlikely to be part of any strategy that could be used to perform either the EFT or the control task: first, spoken words were not part of the stimulus material, and second, the use of verbal working memory was not an appropriate

strategy to cope with our complex visuospatial displays (see Manjaly et al. 2003). Moreover, if language-related components had indeed played a role in our paradigm, one would not have expected the results from our analysis that showed higher left pIFG coupling with left temporo-parietal and left dorsal premotor cortex during the control task than during the EFT. In other words, why should the control task, which was a rather conventional matching task (with minimal visual search), use these putative language-related processes to a stronger degree than the more complex EFT?

We thus conclude that the changes in coupling with left pIFG that we have observed in the areas described above reflect the changes in a general visuospatial network that occur due to different demands of the two tasks on specific visuospatial subprocesses (e.g. direct matching of the target to a “pop-out” element in the control task compared to iterative matching during local search in the EFT). This interpretation is supported by the additional results from our analysis concerning the context-dependent interactions of the second region that was found by Manjaly et al. (2003) to be activated during the EFT relative to the control task, i.e. the left IPS. In contrast to left pIFG, there is much previous evidence that left IPS subserves visuospatial functions (e.g. Hopfinger et al. 2000; Corbetta et al. 2000). In our analysis, the left IPS showed an increased contribution to the right posterior parietal cortex, another “classical” visuospatial area, during EFT compared to the control task (see Fig. 5A). Importantly, in analogy to the findings for left pIFG, the reverse comparison demonstrated higher left IPS coupling with the same left temporo-parietal region during the control task relative to EFT (Fig. 5B).

At a more general level, our findings demonstrate that, depending on the context of the task, left pIFG can contribute to cognitive operations other than

language processing. To some extent, this view had previously been suggested by functional imaging experiments of the human “mirror neuron system”. These studies have demonstrated that the left pIFG is crucially involved in action understanding and action imitation (Binkofski et al. 2001; Buccino et al. 2001; Nishitani & Hari 2001; Rizzolatti et al. 2001). However, although action understanding and imitation do not necessarily constitute language functions in a strict sense, some proposals have tried to bridge these two domains by suggesting that the acquisition of language skills may be linked to the imitation of mouth movements (e.g. Iacoboni et al. 1999; Rizzolatti & Arbib 1998). Therefore, our current findings challenge the traditional view of pIFG as an area entirely dedicated to language much more radically than the results from the above studies of the “mirror neuron system”.

Our results are in accordance with conceptual frameworks in cognitive neuroscience that stress the importance of context and interactivity for understanding the functional architecture of the brain (Friston 1998, 2002; McIntosh 2000). Although these approaches neither deny nor indeed question the existence of specialized computational modules in the brain, they posit that complex cognitive processes cannot be localized to a single region but result from context-dependent interactions within networks of areas. From the opposite perspective, the notion of a distributed architecture of brain function implies that a particular area may be part of different networks depending on a given task context. This view is corroborated by results from neuroanatomical and neurophysiological studies which, collectively, demonstrate that the computational role of any given cortical area cannot be derived from its behavior in a single task or task comparison, but is characterized better through its multivariate response profile across a wide range of tasks (Passingham et al. 2002). This “functional fingerprint” (Passingham et al., 2002) of a particular area critically depends on its unique pattern of anatomical connections with other areas.

This is because the "connectional fingerprint" of an area necessarily constrains its functional interactions, i.e. where it receives information from and where the processed information can be sent to, and thus determines which networks the area can participate in (Kötter & Stephan 2003; Passingham et al. 2002).

The notion that a particular area may contribute to more than one cognitive function by participating in more than one functional network represents a one-to-many structure-function relationship. It should be noted that the opposite principle, i.e. a many-to-one structure-function relationship, is also found in the human brain: there are some cognitive functions which can be mediated by means of different (partially overlapping or totally disjoint) networks (Price & Friston 2002; Friston & Price 2003, Tononi et al. 1999). This concept of "degeneracy" is found at many different biological levels, ranging from the genetic code to the systems level of the brain, and represents a major problem for causal inferences based on behavioral deficits after brain lesions (Price & Friston 2002; Young et al. 2000). Both phenomena, particular areas participating in different cognitive functions and particular cognitive functions being mediated by different networks of areas, bear testimony to the highly distributed architecture of the human brain. Disentangling these complex structure-function relationships will require neurobiologically plausible and mathematically sophisticated models of brain function – a challenge that is only just beginning to be tackled (Friston 2000; Friston et al. 2003; Tagamets & Horwitz 1998).

3. Neurophysiological correlates of relatively enhanced local visual search in autistic adolescents

This chapter contains the following publication:

Manjaly ZM, Bruning N, Neufang S, Stephan KE, Brieber S, Marshall JC, Kamp-Becker I, Remschmidt H, Herpertz-Dahlmann B, Konrad K, Fink GR (2007) Neurophysiological correlates of relatively enhanced local visual search in autistic adolescents. NeuroImage 35: 283-291.

3.1 Summary

Previous studies found normal or even superior performance of autistic patients on visuospatial tasks requiring local search, like the Embedded Figures Task (EFT). A well-known interpretation of this is "weak central coherence", i.e. autistic patients may show a reduced general ability to process information in its context and may therefore have a tendency to favour local over global aspects of information processing. An alternative view is that the local processing advantage in the EFT may result from a relative amplification of early perceptual processes which boosts processing of local stimulus properties but does not affect processing of global context. This study used functional magnetic resonance imaging (fMRI) in 12 autistic adolescents (9 Asperger and 3 high-functioning autistic patients) and 12 matched controls to help distinguish, on neurophysiological grounds, between these two accounts of EFT performance in autistic patients. Behaviourally, we found autistic individuals to be unimpaired during the EFT while they were significantly worse at performing a closely matched control task with minimal local search requirements. The fMRI results showed that activations specific for the local search aspects of the EFT were left-lateralized in parietal and premotor areas for the control group (as previously demonstrated for adults), whereas for the patients these activations were

found in right primary visual cortex and bilateral extrastriate areas. These results suggest that enhanced local processing in early visual areas, as opposed to impaired processing of global context, is characteristic for performance of the EFT by autistic patients.

3.2 Introduction

Autism is a developmental disorder characterized by impaired social interaction and communication as well as by repetitive behaviours and restricted general interests. Over the last decades, several theories have been developed that attempt to explain the cause of autism in terms of dysfunctional central cognitive processes. In addition to theories of impairments in Theory of Mind (Baron-Cohen et al. 2000; Happé 1994) and executive dysfunction (Ozonoff et al. 1991), substantial interest has been devoted to perceptual abnormalities in autism (Behrman et al. 2006). For example, an influential finding in autism research was that autistic patients tend to show superiority for tasks where local processing strategies are beneficial. A classical example of this is the Embedded Figures Task (EFT). Originally devised by Gottschaldt (1926), the EFT involves search for a target figure hidden in complex visual pattern (see Figure 1 for an example). Subjects are required to decide as quickly as possible whether or not the simpler target shape is “hidden” in the complex figure. Shah & Frith (1983) were the first to discover that autistic children responded both faster and more accurately on the EFT compared to matched control children. The initial findings by Shah & Frith (1983) were subsequently replicated by Joliffe & Baron-Cohen (1997) who found both autistic and Asperger children to perform better on the EFT than controls. Other studies found non-significant differences in the behavioral performance of patients and controls on the EFT (Brian & Bryson 1996; Ring et al. 1999; Ropar & Mitchell 2001), but even this is remarkable given that

autistic patients usually tend to perform worse than controls on most complex cognitive tasks. This behavioral advantage (absolute or relative, depending on the study) of autistic patients on the EFT has been interpreted in two major ways: (i) in terms of "weak central coherence" (WCC; Frith 1989; Shah & Frith 1983; Happé 1999; Hill & Frith 2003; Joliffe & Baron-Cohen 1997) and (ii) from the perspective of theories that postulate enhancements of early perceptual processes in autism (Mottron et al. 2006; Plaisted et al. 2003).

Central coherence describes the ability to integrate separate pieces of information into meaningful wholes. In relation to autism, the WCC theory postulates a general (domain-unspecific) tendency to favour processing of local stimulus properties due to a reduced ability in processing global context (Frith 1989; Happé 1999). It assumes that WCC occurs at both “low” and “high” levels of information processing. Low-level WCC refers to the tendency to neglect context in the sensory (e.g. visual) domain, favouring the processing of individual stimulus features, whereas high-level WCC concerns impairments of more abstract contextual processes (Happé 1996; Joliffe & Baron Cohen 1997). WCC is not necessarily always a cognitive limitation but should actually be advantageous for perceptual tasks which require processing of local aspects of complex stimuli, like the EFT (Shah & Frith 1983; Happé 2001).

According to the classical WCC theory, superior performance of autistic patients in local processing during the EFT results from a deficiency of global context processing. However, some studies using hierarchically structured stimuli suggested that autistic patients respond to the global stimulus level with similar efficiency as controls (Mottron et al. 1999, 2003; Ozonoff et al. 1994; Plaisted et al. 1999, 2003). These findings imply that autistic patients might not necessarily show a deficiency in

global context processing with resulting superior local processing but could instead have a primary superiority in local processing, with global processing being unaffected. Such a perspective has been formulated with a strong focus on perception, most prominently by Plaisted and colleagues (Plaisted et al. 1998; O'Riordan & Plaisted 2001; Plaisted et al. 2003) and Mottron and Burack (Mottron & Burack 2001; Mottron et al. 2006). Plaisted and colleagues have suggested that atypical perceptual processes in autism enhance the salience of individual stimulus features without compromising global processing. Their experiments suggested that this enhancement occurs at very early stages of sensory processing hierarchies (Plaisted et al. 1998; O'Riordan & Plaisted 2001; Plaisted et al. 2003). A related, although not identical, account of abnormal perception in autism is provided by the Enhanced Perceptual Functioning (EPF) theory (Mottron & Burack 2001; Mottron et al. 2006). According to this theory, low-level perceptual processing is abnormally enhanced relative to high-level cognitive processes, making automatic perceptual processes more difficult to control by top-down mechanisms and thus more likely to supersede or interfere with higher cognitive processes. Neurophysiologically, this abnormality is proposed to be reflected by a general "skewing" of brain activation towards primary sensory areas in autistic patients, providing the basis of a superior "perceptual trace" that enhances memory for local stimulus properties and thus might explain the good performance of autistic patients on the EFT (Mottron et al. 2006).

So far, there is little neurophysiological evidence that would help distinguishing between the WCC theory and its alternatives. For each theory, predictions can be derived concerning the differences in brain activity between a task requiring local visual search (like the EFT) and a similar control task with reduced local search requirements. Notwithstanding their subtle differences, the theories by Plaisted and Mottron & Burack, respectively, both postulate that early visual areas, whose small

receptive field sizes are appropriate for perceptual processing of local stimulus properties, should show higher activation in patients compared to controls. For the classical WCC theory, precise predictions about the sites of differential activations during the EFT have not been formulated in detail before but can be derived on the basis of recent studies. It is well-established that several left-hemispheric areas beyond extrastriate cortex like the IPS (Weissman & Woldorff 2005) are crucial for processing local stimulus properties, despite relatively large receptive fields. In contrast, global stimulus properties are predominantly processed by right-hemispheric areas (Hellige 1996; Martinez et al. 1997; Proverbio et al. 1998; Robertson & Lamb 1991; Weissman & Woldorff 2005; Yamaguchi et al. 2000). For early visual areas with small receptive fields (see above), such a lateralisation is more controversial (Fink et al. 1996, 1997; Sasaki et al. 2001; Weissman & Woldorff 2005). Therefore, contrasting a task with strong local processing requirements like the EFT to a control task with similar stimuli but minimal local processing requirements, one would expect left-lateralized activations which may or may not include early visual cortices, but should definitely be observed for "higher" areas, particularly the IPS (Weissman & Woldorff 2005). This is exactly what we found in a previous study of adults where the local processing requirements of the EFT activated the left IPS and the left inferior frontal gyrus (IFG; Manjaly et al. 2003). Critically, since the WCC theory assumes deficient global processing, it would predict attenuated right-hemispheric activity and that the lateralization of activity during the EFT to left IPS and left IFG should be more pronounced in autistic subjects than in controls. So far, the only neuroimaging study of the EFT in autism is an fMRI study by Ring et al. (1999). Unfortunately, this study had a small sample size (six patients) and only compared EFT against rest (fixation), therefore the activations are relatively unspecific and not easily interpretable.

The present study aimed at providing more specific neurophysiological evidence to distinguish between the different theories of autism. Our recently established EFT paradigm (Manjaly et al. 2003) contrasts the EFT with a closely matched visuospatial control task (CT) with very similar stimuli but minimal local search requirements, as well as with a simple shape recognition task. This paradigm was combined with fMRI to measure brain activity in age- and IQ-matched groups of children with autistic spectrum disorders and control children in order to determine whether the EFT-specific activations would support the WCC theory or the perceptual theories by Plaisted and Mottron & Burack, respectively.

3.3 Methods

3.3.1 Subjects

12 right handed adolescents with the diagnosis of Asperger syndrome (n=9) or High-Functioning Autism (HFA; n=3) and a mean age of 14.4 years (SD = 2.7 years) were studied in comparison to 12 controls (14.3 $\pm$ 2.7 years) without any history of neurological or psychiatric illness. Since the majority of studies suggest that both, HFA and Asperger syndrome, belong to the same spectrum disorder (Gilchrist et al. 2001; Frith & Happé 2005), we decided to include either patients with HFA or Asperger syndrome in the autistic group. The two groups were matched for gender, age, handedness, and IQ as measured with the Culture Fair Intelligence Test 20 (CFT 20, Weiß 1998). All children and their parents or caregivers gave their written informed consent after having been informed about the details and the purpose of this study. The study was approved by the ethics committee of the University Hospital Aachen.

The autistic children were diagnosed by experienced clinicians according to the standard criteria of ICD-10 (World Health Organization, 1993) and DSM-IV (American

Psychiatric Association, 1994) and underwent extensive psychiatric examination. The expression of autistic symptoms was further assessed by the German version of the Autism Diagnostic Observation Scale (ADOS-G; Lord 2000) and a semi-structured autism specific parent interview (ADI-R; Le Couteur et al.1989); this in-depth assessment was conducted by trained examiners (N.B., I. K.-B.). Subjects with Asperger syndrome had an IQ above 80, met DSM-IV criteria for Asperger syndrome or autism and fulfilled the cut-off criteria of the ADOS-G and ADI-R for autism or autism spectrum disorder. Subjects with HFA fulfilled ADI-R and ADOS-G threshold scores for autism, but had an IQ of at least 80, and a history of phrase speech development at 36 months or older. Since many persons with Asperger syndrome also meet ADI-R and DSM-IV criteria for autism (e.g. Mayes et al. 2000) the primary distinguishing feature between individuals with HFA and Asperger syndrome was a history of clinically significant language impairment (see also Howlin, 2003). Additionally, all parents of the autistic group completed the German version of the Autism Screening Questionnaire (ASQ; Bölte et al., 2000). To exclude clinically relevant psychopathology, the Child Behaviour Checklist (CBCL; Achenbach & Edelbrock 1983) was completed by all parents in both groups. None of the subjects showed any relevant somatic or psychiatric disorder except autism in the clinical group. Table 1 summarizes the major clinical and demographic data. To minimize movement artefacts and to prevent anxiety in the unfamiliar surroundings, all subjects were familiarized to the fMRI scanner environment using a simulated ("mock") MRI scanner that looked and sounded similar to the real scanner.

Table 1: *Demographic and clinical data of the subjects in this study.*

	Controls	Autism	p
	mean (range; SD)	mean (range; SD)	
N	12	12	
Age (years)	14.3 (10-18; 2.7)	14.4 (10-17; 2.8)	.94
IQ (CFT-20)	109.3 (83-132; 13.6)	110.1 (83-134; 20.0)	.92
Handedness	12 right-handed	12 right-handed	
DSM-IV/ ICD-10 Diagnosis			
Asperger's syndrome	0	9	
High- functioning Autism (HFA)	0	3	

3.3.2 Stimuli and experimental design

In a previous study (Manjaly et al. 2003), we established an fMRI-compatible EFT version for adults. This version turned out to be too difficult and too long for young adolescents, particularly patients. For the present study, we therefore adapted our version of the EFT. Using a PC graphics program (Corel Draw 9.0, Corel Inc.), 12 figures of comparable complexity were created that consisted of the same number of lines (8). Each of these stimuli was presented eight times in the experiment, four times in the EFT condition and four times in the control task (CT, see below), resulting in 48 trials per condition. On each trial, a target figure was displayed next to

the complex figure (50% left, 50% right). In 50% of all trials the accompanying target figure was embedded in the complex figure ("correct" target figure) and in 50% it was not ("incorrect" target figure). To prevent priming effects, each correct target figure was only presented once throughout the experiment. Because the incorrect target figures were not embedded in any complex figure shown in the experiment, they could safely be used twice, i.e. once each in EFT and CT. Figure 1 shows examples of the stimuli used in the EFT and the CT.

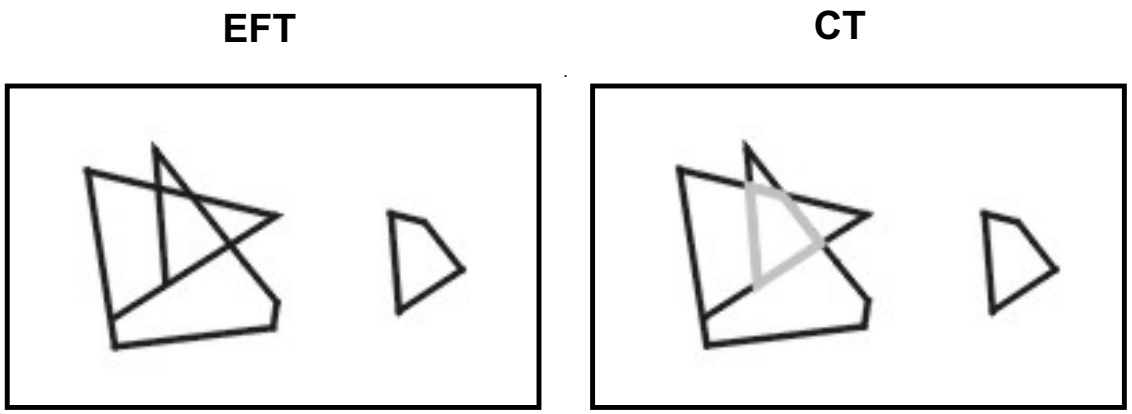

Figure 1: Two examples of the stimuli used for the Embedded Figures Task (EFT) and the control task (CT).

In the EFT, subjects had to decide whether or not the target figure matched any subpart of the complex figure. Crucially, the EFT requires one to dissect the complex figure into local substructures in order to decide whether any of them matches the target figure. To control for other cognitive processes involved in the EFT, e.g. more general aspects of visual search and perception of complex geometric figures, we used a control task (CT) which comprised all cognitive aspects of the EFT but had minimal local visual search requirements. In this CT, a substructure of the complex figure was highlighted with a grey line, and subjects had to decide if the outlined substructure was the same as the simultaneously presented target figure or not. As

a further control, we used a high-level baseline (BL) in which subjects were presented with a triangle or a square and had to discriminate between them. This shape recognition task controlled for aspects common to both EFT and CT, i.e. visual recognition and attention, decision-making and motor responses, but did not involve any visuospatial search or matching processes. Overall, our paradigm thus had a hierarchical structure, with the CT controlling for all aspects of the EFT except the significant local visual search component, and the BL controlling for more basic cognitive and motor processes present in both EFT and CT. In our previous study (Manjaly et al. 2003), stimuli during EFT and CT were presented either horizontally or vertically. Since we did not find any significant task-by-orientation interaction in that previous experiment, we only used a horizontal arrangement of stimuli in the present study.

All answers were recorded via button presses, using MRI-compatible key pads. Stimuli were presented in black on a white background on a 30 x 15 cm screen (horizontal visual angle of 42.3º, vertical visual angle of 24.4º) for 3000 ms (stimulus on-time, SOT) with an inter-stimulus interval (ISI) of 1000 ms (blank screen) using Presentation 7.96 (Neurobehavioral Systems Inc., San Francisco). SOT and ISI were identical for all conditions. Subjects viewed the display from a distance of 33 cm (20 cm screen to mirror, 13 cm mirror to subjects´ eyes). The complex figure and target figure combined covered a visual angle of 16.9º horizontally and 3.5º vertically (combined stimulus width 10cm, height 2 cm). In 50% of the trials the target appeared left and the complex figure appeared right ; in the other 50% of the trials these positions were reversed. We controlled for order effects by (i) counterbalancing the condition order across subjects and by (ii) randomizing the order of stimuli across blocks and conditions for each subject.

A blocked design was adopted in order to maximize statistical efficiency. Blocks from all conditions consisted of 6 trials, and each block lasted 24 seconds, preceded by a short instruction screen (6 seconds). The experiment consisted of 8 EFT blocks, 8 CT blocks, and 16 BL blocks, giving a total scanning time of 16 minutes.

Reaction times and error rates were recorded as behavioural measures. Subjects were instructed to respond as quickly and as accurately as possible in all tasks. In all conditions, the number of required "yes" and "no" responses was 50% each. The subjects' condition-specific mean reaction times and mean error rates of all two experimental runs were compared by analysis of variance (ANOVA), using SPSS V11 (SPSS Inc., Chicago, IL).

3.3.3 MRI acquisition

Echo Planar Imaging was performed on a Siemens Sonata 1.5 Tesla scanner using a standard head coil. Pulse sequence parameters were as follows: TE = 66 ms; TR = 3.02s; FOV = 200 x 200 mm; θ = 90°; matrix size = 64 x 64; pixel size = 3.125 x 3.125 mm; slice thickness = 4.0 mm; inter-slice gap = 0.4 mm; 30 slices. Additionally, we obtained high-resolution, T1-weighted structural brain images using a standard MP-RAGE (magnetisation-prepared, rapid acquisition gradient echo) sequence.

3.3.4 fMRI data analysis

All calculations and image manipulations were performed on Sun Ultra 60 workstations (SUN Microsystems Computers) using MATLAB 6.5 (The Mathworks Inc., Natick, MA, USA) and SPM2 (Statistical Parametric Mapping, SPM; Wellcome Department of Imaging Neuroscience, London, UK).

For each subject, the first five images were discarded, the remaining 320 images were realigned to the first image to correct for head movements, spatially

normalised, i.e. transformed into a standard stereotactic space as defined by the MNI template (Montreal Neurological Institute) using a non-linear warping algorithm (Ashburner & Friston 1999), and resampled to a voxel size of 3 x 3 x 3 mm. The normalised scans from each subject were smoothed with a three-dimensional Gaussian kernel of 10 mm full width half maximum for the group analysis to meet the statistical requirements of the General Linear Model and to compensate for remaining inter-individual variability in anatomy across subjects.

Data were analyzed using a general linear model in SPM2, removing subject-specific low frequency signal drifts by a high pass filter of 128 sec. The different conditions were modelled by convolving box car functions with a canonical haemodynamic response function. In addition to regressors modelling the three different tasks and the instruction periods, we included six regressors in the design matrix that consisted of the realignment parameters, describing rotation and translation of the subject's head during the experiment. This allowed us to regress out any variance that could be explained by a linear combination of head translations and rotations. After estimation of the model parameters, specific effects were tested for by applying appropriate linear contrasts to the parameter estimates, resulting in contrast images. Specifically, we computed contrasts for each relevant task pair, i.e. EFT>CT, CT>EFT, EFT>BL, CT>BL.

Subsequently, contrast images were entered into second-level t-tests (one-sample t-tests for within-group analyses, two-sample t-tests for between-group analyses), implementing random effects group analyses (Penny & Holmes 2004). These analyses, which used the non-sphericity correction of SPM2 to take into account potential group differences in variance, resulted in a t-statistic for each voxel. The significance of local topological features of the resulting SPM{T} can be

determined using Gaussian random field theory. In all analyses, areas of activation were identified as significant only if they passed a threshold of $p< 0.05$, corrected for multiple comparisons at the cluster level (Poline et al. 1996), using a standard $p<0.001$ cut-off at the voxel-level.

In addition to the specific contrasts of interest, we also tested for the overall effect of visual analysis of complex geometric figures with differing degrees of local search relative to pure recognition of geometric shapes. For this purpose, we performed a random effects conjunction analysis, based on inclusive masking, as suggested by Nichols et al. (2005). This conservative analysis corresponds to a logical AND operation, showing those voxels which are significant in both the EFT>BL and CT>BL comparisons in both patients and controls (Figure 3). For this analysis we used a threshold of $p<0.05$, corrected for multiple comparisons at the voxel level.

3.4 Results

3.4.1 Behavioural measures

We analysed both reaction times (RTs) and the percentage of correct (PC) responses across all volunteers using a two-factorial ANOVA with factors “task” (EFT vs. CT) and “group” (patients vs. controls) and Greenhouse-Geisser correction for non-sphericity. Reaction times were computed for correct responses only. The results are summarized by Table 2.

Table 2: *Behavioural results of both groups on the Embedded Figures Task (EFT), Control Task (T) and the baseline condition (BL)*

	Patients (N=12)			**Controls (N = 12)**		
	mean	SE	range	mean	SE	range
RT BL [ms]	683	99	439-1559	694	51	448-1032
RT CT [ms]	1435	102	993 - 2236	1288	49	1119 - 1661
RT EFT [ms]	1825	83	1331 – 2188	1834	56	1545 – 2222
% correct CT	94.1	2.6	68.75 - 100	97.7	0.8	91.67 - 100
% correct EFT	85.6	2.5	68.75 – 93.75	89.9	1.6	79.17 – 95.83

As expected, the analysis of RTs showed a main effect of task, i.e. pooled across groups responses were faster for the CT (1362 ± 57 ms [mean ± standard error]) than for the EFT (1829 ± 50 ms) ($p < 0.001$). In contrast, there was no main effect of group, i.e. pooled across tasks the RTs in the autistic group (1630 ± 86 ms) were not significantly different from the controls (1561 ± 50 ms) ($p = 0.496$). However, while there was virtually no difference between groups for the EFT (patients: 1825 ± 83 ms; controls: 1834 ± 56 ms; $p = 0.9$), patients took numerically longer to respond during the CT than the controls (patients: 1435 ± 102 ms; controls: 1288 ± 49 ms; $p = 0.2$) (see Figure 2), and the resulting task-by-group interaction was at the borderline of significance ($p = 0.054$).

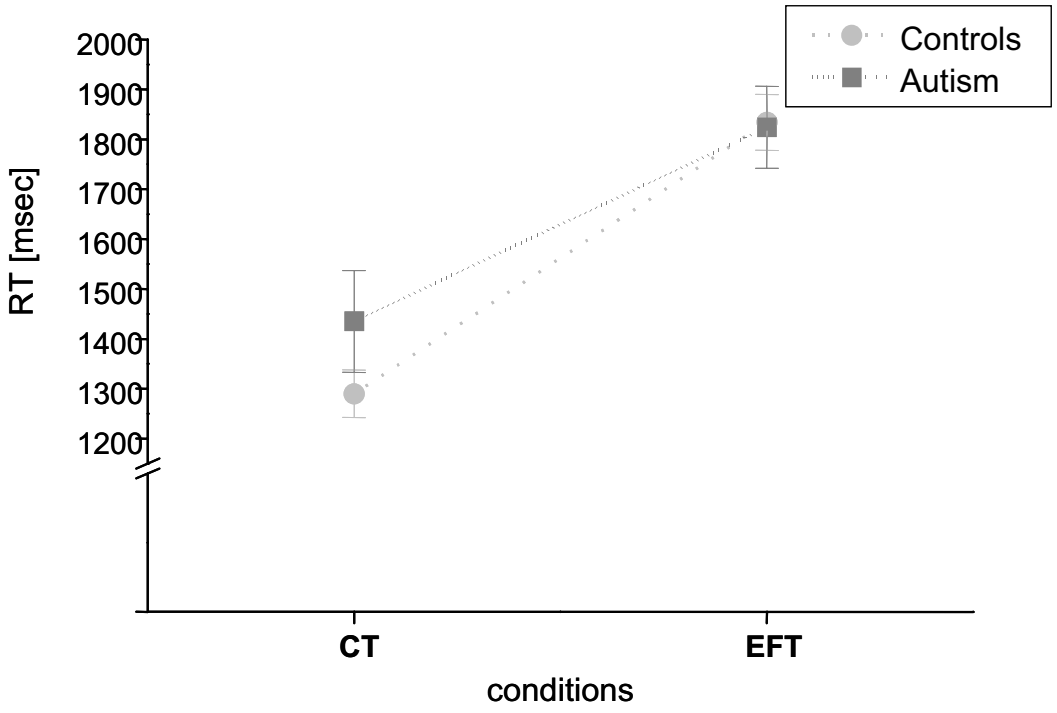

Figure 2: Mean reaction times (in ms) of both the patient and control group for EFT and CT. Error bars denote standard errors. Patients and controls are almost identical in their reaction times in the EFT, whereas patients respond much more slowly than controls in the control task. This group x condition interaction was bordering significance ($p = 0.054$).

Analysing the percentage of correct responses (PC), again a significant main effect of task was found, i.e. pooled across groups subjects made more correct decisions for the CT (95.9 ± 1.4 %) than for the EFT (87.8 ± 1.5 %) ($p < 0.001$). There was no main effect of group, i.e. pooled across tasks the proportion of correct responses in the patient group (89.8 ± 2.3 %) was not significantly different from that in the control group (93.8 ± 1.1 %) ($p = 0.126$). In contrast to the RT data, there was no task-by-group interaction ($p = 0.805$).

3.4.2 fMRI results

Initially, we determined the areas that were activated, in both patients and controls, for visual processing of complex geometric figures as compared to simple shape

recognition. For this purpose, we used a conjunction analysis that was based on inclusive masking of the contrasts EFT > BL and CT > BL (Nichols et al. 2005). This "logical AND" conjunction analysis revealed that both autistic subjects and control subjects showed activations, for contrasting both EFT and CT against BL, in the middle occipital gyrus and the intraparietal sulcus bilaterally, as well as activations in right fusiform gyrus, right inferior occipital gyrus, left lingual gyrus, left superior parietal gyrus, right anterior insula and left thalamus ($p < 0.05$, corrected; see Figure 3 and Table 3 for coordinates of the maxima).

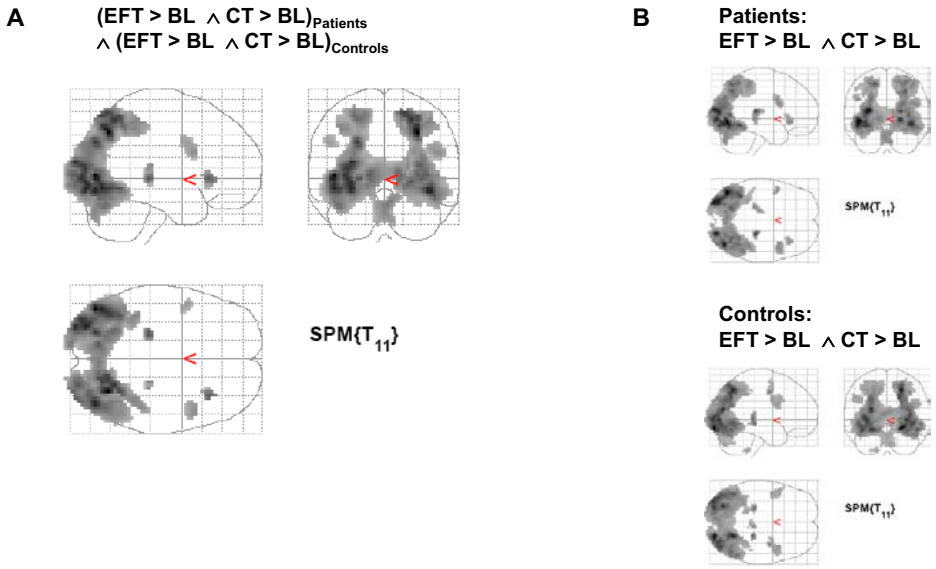

Figure 3: Random effects conjunction analysis, based on inclusive masking, which shows those clusters that are significant in both the EFT>BL and CT>BL comparisons, across both groups. This analysis tests for the overall effect of visual search in geometric figures (EFT and CT) relative to pure recognition of geometric shapes (baseline condition, BL), in both patients and controls. Results are thresholded at $p<0.05$ at the voxel level, corrected for multiple comparisons across the whole brain.

Table 3: *Conjunction analysis* $(EFT > BL \ \wedge CT > BL)_{Patients} \wedge (EFT > BL \ \wedge CT > BL)_{Controls}$ *of the fMRI data*

	Side	x	y	z	k
Middle occipital gyrus	left	-45	?78	3	173
	right	24	-93	-3	4
	right	33	-84	12	4
	right	30	-99	3	1
Intraparietal sulcus	right	30	-66	42	72
	left	-24	-78	33	10
Fuisform gyrus	right	39	-78	-12	33
Inferior occipital gyrus	right	39	-93	3	4
Lingual gyrus	left	-12	-75	3	4
Thalamus	left	-24	-30	0	2
Superior parietal gyrus	left	-27	-60	57	1
Anterior insula	right	33	24	0	1

Table 3: This table lists the results from the conjunction analysis (implemented by inclusive masking) shown by Fig. 11. All results are significant at p<0.05 at the voxel level, corrected for multiple comparisons across the whole brain. Note that because of the multiple masking involved in this analysis, it is not meaningful to list individual T scores. k = number of activated voxels; x,y,z = coordinates of local maxima in MNI space.

More importantly, however, was the difference in activation during performance of the EFT in comparison to CT, separately in both groups. All results reported below are significant at the cluster-level (p<0.05), corrected for multiple comparisons across the whole brain. The coordinates and T-values given below refer to the local maxima of

the significant clusters. Assessing the EFT vs. CT contrast in the control group showed an activation in left posterior parietal cortex (maximum at x = -12, y = -72, z = 57; T = 6.88) and left dorsal premotor cortex (-24, -3, 63; T = 6.27; see Figure 4 and Table 4). This activation pattern is a fairly good replication of our previous results when testing adult volunteers on the EFT (Manjaly et al. 2003); see Discussion. The reverse contrast, i.e. CT>EFT, demonstrated an activation in the left medial temporal lobe (-27, -18, -18; T = 9.18).

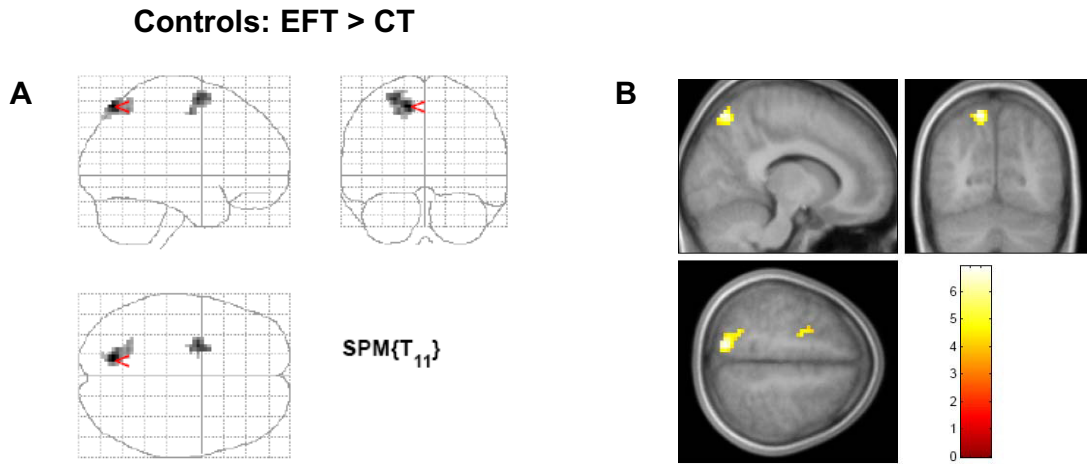

Figure 4: Random effects analysis of the EFT>CT contrast within the control group. This analysis tests for effects specific for the local visual search processes required by the EFT but not by the otherwise closely matched CT. (A) Maximum intensity projection of significant clusters. Results are thresholded at p<0.001 and are cluster-level corrected for multiple comparisons across the whole brain at p<0.05. (B) The SPM{T} overlaid on the mean structural image of the group. The colour bar indicates T-values.

Table 4: *fMRI results: EFT > CT, separately in the autistic and the control group*

Controls	Side	x	y	z	T score	k
Posterior parietal cortex	left	-12	-72	57	6.88	86
Dorsal premotor cortex	left	-24	-3	63	6.27	67
Autistic						
Calcarine sulcus	right	9	-72	6	5.83	54
Cerebellum	right	6	-69	-33	5.88	46
Extrastriate cortex	right	39	-81	9	6.79	46
Extrastriate cortex	left	-27	-90	3	6.51	83

Table 4: This table lists the significant clusters shown by Figs. 12 & 13, with coordinates referring to the local maxima of the clusters. k = number of activated voxels; x,y,z = coordinates in MNI space; $p < 0.05$, corrected for multiple comparisons at the cluster level, using a cut-off of $p<0.001$ at the voxel-level.

The group of autistic subjects revealed a different activation pattern (see Figure 5 and Table 4). When comparing EFT to CT, significant activations were found in the left (-27, -90, 3; T = 6.51) and right (39, -81, 9; T = 6.79) extrastriate cortex, in the cortex around the right calcarine sulcus (9, -72, 6; T = 5.83), and in the right cerebellar hemisphere, extending into the vermis (6, -69, -33; T = 5.88). When comparing the locations of the activations in visual areas against a probabilistic cytoarchitectonic atlas (http://www.bic.mni.mcgill.ca/cytoarchitectonics) that was warped into MNI space (see Eickhoff et al. 2005 for the methodology), we found that

the local maximum of the activation in the vicinity of the right calcarine sulcus (9, -72, 6) had a high probability (80%) of being located in area V1. In contrast, the two local maxima of the activations in left and right extrastriate cortex had zero percent probability of being located in either V1 or V2. The reverse task comparison, i.e. CT>EFT, did not show any significant activation in the patient group.

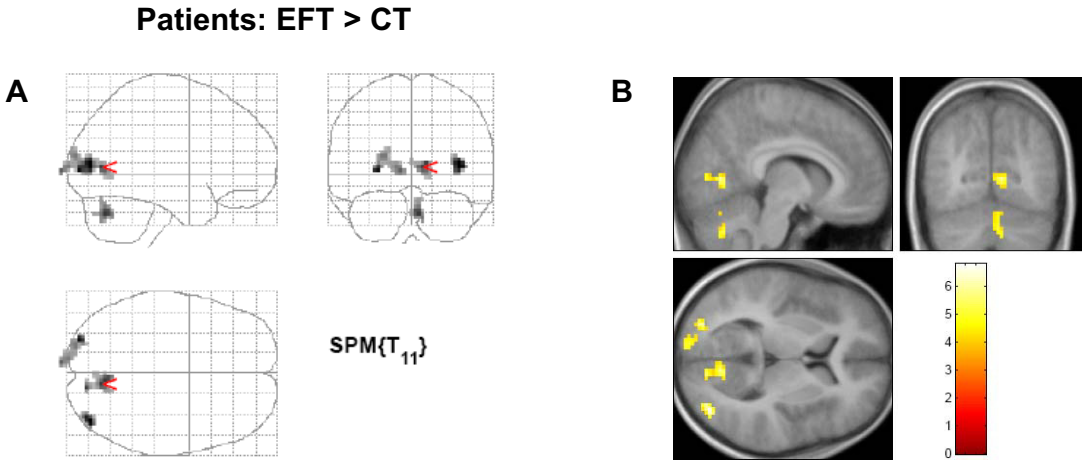

Figure 5: Random effects analysis of the EFT>CT contrast within the patient group. See Fig. 12 for further explanations.

In a next step, we assessed whether there were any brain regions in which the difference between EFT and CT was significantly different between patients and controls. This corresponds to testing for group-by-condition interactions, which can be implemented by a two-sample t-test operating on the within-group contrast images. This analysis did not yield any results that were significant after correcting for multiple comparisons across the whole brain. However, at uncorrected levels of significance, some of the regions (e.g. calcarine sulcus and right extrastriate cortex) which were significantly activated in the EFT vs. CT contrast in the autistic group, also showed such an interaction, i.e. higher EFT vs. CT differences in the autistic than in the control group (see Fig. 6).

A **Primary visual cortex**
x = 9, y = -72, x = 6
p < 0.013

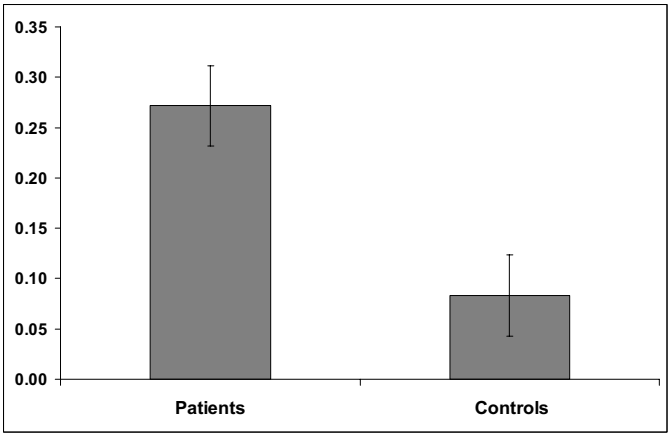

B **Right extrastriate cortex**
x = 39, y = -81, x = 9
p < 0.028

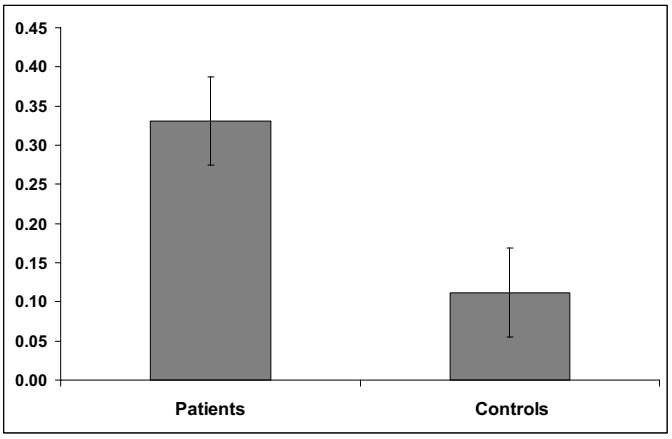

Figure 6: This bar plot shows the contrast values for the EFT >CT contrast for several regions selected from the analysis in Fig. 13, averaged across subjects. The values correspond to the percent signal change, relative to the global brain mean signal. Error bars denote the standard error. Although the EFT vs. CT parameter difference is larger in the patient group compared to controls, and this difference is significant ($p < 0.05$) at the level of the individual voxels studied in primary visual (A) and right extrastriate cortex (C), it did not survive correction for multiple comparisons.

3.5 Discussion

Compared to previous work, the present study is, to our knowledge, the first to simultaneously assess behavioural performance on an additional visual task (CT) that closely matches the EFT in all cognitive processes except the major local visual processing component itself. While our behavioral results do not support the notion that autistic patients have an *absolute* advantage for local visual processing, they do suggest that autistic individuals have a *relative* advantage for local processing. This was reflected by a task-by-group interaction ($p = 0.054$) in terms of RTs. This

interaction indicated that autistic patients were equally fast on the EFT as the control subjects (Table 2; note that error rates were also very similar), but showed slower responses on the CT where local processing requirements were minimal. How does this finding fit with previous behavioural studies of EFT performance by autistic and control subjects? In the classical study by Shah & Frith (1983) as well as in the study by Joliffe & Baron-Cohen (1997) autistic children were found to respond both faster and more accurately than control children. This superior performance of the autistic group was consistent with the findings of Kagan & Kogan (1970) who found an inverse relation between sensitivity to social cues and performance on the EFT in children. Similarly, Baron-Cohen et al. (1997) reported that parents of children with Asperger syndrome were significantly faster on the EFT than a control group of parents with non-autistic children. Several other studies provided additional evidence for better performance of of autistic patients in detecting embedded figures (de Jonge et al. 2006; Jarrold et al. 2005; Pellicano et al. 2006). Two other studies, however, deviated from this pattern. Ropar & Mitchell (2001) found that autistic and Asperger children performed equally well on the EFT as control children. A study by Brian & Bryson (1996) also failed to find superior performance of autistic patients compared to controls. The latter study, however, is difficult to interpret because the groups differed in age.

The current study achieved a fairly good replication of our previous fMRI results of adult volunteers performing the EFT (Manjaly et al. 2003). In that study contrasting EFT to CT revealed significant activations in the left posterior parietal cortex, including the IPS, and in the left ventral premotor cortex (posterior IFG). This finding is consistent with the well-established left-hemispheric dominance for local visual processing (see Introduction). Using a probabilistic cytoarchitectonic atlas, the premotor activation was found to overlap with areas 44 and area 6. A subsequent

connectivity analysis demonstrated that this activation functionally interacted with areas commonly involved in visuospatial processing (Manjaly et al. 2005). In the present study, comparing EFT to CT in the control group activated the left IPS and the left dorsal premotor cortex. While the parietal activation reported here was very similar to the one found by Manjaly et al. (2003), the premotor activation was more dorsally located. This may be due to differences in local processing in adults and adolescents, or it may result from differences in the design of the two studies. For example, the stimuli used by the current study were less complex (eight instead of twelve composing lines) and were shown in horizontal orientation only.

Importantly, the patient group showed a different activation pattern when comparing EFT to CT. Here, we did not find a further increase in the left-lateralisation of activity in IPS and other "higher" areas as implied by the classical WCC theory (see Introduction). Instead, activations were found in the cortex surrounding the right calcarine sulcus and in the extrastriate cortex bilaterally. These activations at the early stages of visual processing in autistic individuals are compatible with the hypotheses by Plaisted et al. and Mottron & Burack, respectively, that the advantage of autistic patients for local visual processing may be due to differences in basic perceptual processes. According to Plaisted et al., in the early sensory cortices of autistic patients the salience of individual stimulus features is boosted without compromising processes of global integration (Plaisted et al. 1998; O'Riordan & Plaisted 2001; Plaisted et al. 2003). Similarly, the EPF theory by Mottron and Burack holds that superior perceptual processing and enhanced "perceptual traces" in early visual cortex could induce better memory for local properties of visual stimuli (Mottron & Burack 2001). In a recent review of the evidence for this, Mottron et al. (2006) suggested that enhanced V1 activation may be a general phenomenon for visual tasks in autism. Finally, we also found an

activation in the right cerebellar hemisphere, extending into the vermis, which is neither predicted by the WCC theory nor by the other theories. Currently, we cannot offer a good explanation for this finding.

The direct group comparison between patients and controls for the EFT vs. CT contrast did not yield any brain regions with between-group differences in local processing that were significant at $p < 0.05$ corrected. However, at uncorrected levels of significance, some of the regions (e.g. the calcarine sulcus) which were significantly activated in the EFT vs. CT contrast in the autistic group, also showed a task x group interaction, i.e. higher EFT vs. CT differences in the autistic group compared to the control group (see Fig. 6).

One limitation of our study is the restricted sample size. Even though we studied twice as many patients (12) than the only other EFT fMRI study in autism available so far (Ring et al. 1999), this is still a limited number given recent evidence that there may be considerable variance with regard to EFT performance among patients with autistic spectrum disorder (Edgin & Pennington 2005). Ideally, one would subdivide the patients into subgroups with different performance levels on the EFT. With the current sample size, however, this was not feasible statistically. This approach is suggested for future studies with larger sample sizes, and the present findings should be treated as preliminary results until confirmed in larger samples.

Notwithstanding the above caveats, our present results, which point to differential information processing at early stages of visual perception in autism, are in line with evidence from a growing body of psychophysical, electrophysiological and fMRI studies (reviewed by Plaisted et al. 2003 and Mottron et al. 2006). For example, the psychophysical experiments by Bertone et al. (2005) and Caron et al. (2006) pointed to differences in processing orientation information and perceptual

cohesiveness of visual stimuli, respectively, at the level of early visual areas in autistic patients. McPartland et al. (2004) demonstrated an abnormal N170 event-related potential at early stages of face processing. Brown et al. (2005) reported abnormal EEG gamma activity over visual cortex, possibly reflecting a diminished signal-to-noise ratio due to decreased inhibitory processing at the early stages of perception in autism. Koshino et al. (2005) reported increased activity in extrastriate areas of autistic patients, compared to controls, during a visual N-back working memory task studied with fMRI. Belmonte & Yurgelun-Todd (2003) applied fMRI to a simple visuospatial attention task and found activations in primary visual and ventral occipital cortex of autistic subjects, but not of controls.

Concerning local visual search in particular, so far only one previous study has examined the neural mechanisms underlying local visual processing in autistic patients (Ring et al. 1999). This fMRI study investigated six autistic subjects and twelve controls, contrasting the EFT with an unspecific 'fixation only' condition. When comparing the EFT-related activations between groups, Ring et al. found that the only regions exhibiting higher activity in the autistic group were primary and secondary visual areas. The far more specific EFT vs. CT contrast in our study produced results for the autistic group that are compatible with the findings by Ring et al. (1999).

The present study included a carefully designed control condition (CT) for a task probing local visual processing (EFT). However, it should be noted that while this task controlled for all motor, cognitive, and perceptual processes (except local visual search) of the EFT, it did not directly probe the capacity for global integration. A next step therefore is to directly compare with fMRI local and global processing capacities in larger samples of autistic patients, e.g. using identical, hierarchically structured

stimuli (Rinehart et al. 2000; Fink et al. 1997). In addition, future studies should focus on the direct comparison between different childhood psychiatric disorders characterized by attentional problems in order to clarify how specific these cognitive profiles are for patients with autism.

4. References

Abell F, Krams M, Ashburner J, Passingham R, Friston K, Frackowiak R, Happe F, Frith C, Frith U. The neuroanatomy of autism: a voxel-based whole brain analysis of structural scans. Neuroreport 1999; 10:1647-1651.

Achenbach TM, Edelbrock C. Manual for the Child Behavior Checklist and Revised Child Behavior Profile. Burlington: University of Vermont, Department of Psychiatry 1983.

American Psychiatric Association. Diagnostic and statistical manual of mental disorders (IV). American Psychiatric Association, Washington, DC; 1994.

Amunts K, Schleicher A, Bürgel U, Mohlberg H, Uylings HB, Zilles K. Broca's region revisited: cytoarchitecture and intersubject variability. J Comp Neurol 1999; 412: 319-341.

Asperger H. Die autistischen Psychopathien im Kindesalter. Archiv für Psychiatrie und Nervenkrankheiten1944; 117:76-136

Ashburner J, Friston KJ. Nonlinear spatial normalization using basis functions. Human Brain Mapping 1999; 7 254-266.

Baird G, Charman T, Baron-Cohen S, Cox A, Swettenham J, Wheelwright S, Drew A. A screening instrument for autism at 18 months of age: a 6 year follow-up study. J. Am. Acad. Child Adolescent Psychiatry 2000; 39: 694-702.

Baron-Cohen S, Hammer J. Parents of children with Asperger syndrome: what is the cognitive phenotype? J Cogn Neurosci 1997. 9: 548-554.

Baron-Cohen ST, Tager-Flusberg H, Cohen DJ. Understanding other minds. Perspectives from autism. Oxford: Oxford University Press 1993

Baron-Cohen ST, Tager-Flusberg H, Cohen DJ. Understanding other minds. Perspectives from developmental cognitive neuroscience. Oxford: Oxford University Press 2000.

Baron-Cohen S, Belmonte MK. Autism: A window onto the development of the social and the analytic brain. Annu. Rev. Neurosci. 2005; 28:109-126.

Belmonte MK, Yurgelun-Todd DA. Functional anatomy of impaired selective attention and compensatory processing in autism. Brain Res Cogn Brain Res 2003; 17: 651-664.

Benson DF. Aphasia, Alexia, and Agraphia. Churchill Livingstone, New York 1979.

Bentley P, Husain M, Dolan RJ. Effects of cholinergic enhancement on visual stimulation, spatial attention, and spatial working memory. Neuron 2004; 41(6): 969-982.

Bertone A, Mottron L, Jelenic P, Faubert J. Enhanced and diminished visuo-spatial information processing in autism depends on stimulus complexity. Brain 2005; 128: 2430-2441.

Bihrle AM, Belugi U, Delis D, Marks S. Seeing either the forest or the trees. Brain and Cognition 1989; 11: 37-49.

Binder JR, Frost JA, Hammeke TA, Cox RW, Rao SM, Prieto T. Human brain language areas identified by functional magnetic resonance imaging. Journal of Neuroscience 1997, 17: 353-362.

Binkofski F, Amunts K, Stephan KM, Posse S, Schormann T, Freund HJ, Zilles K, Seitz RJ. Broca's region subserves imagery of motion: a combined cytoarchitectonic and fMRI study. Human Brain Mapping 2001; 11: 273-285.

Boelte S, Crecelius K, Poustka F. Der Fragebogen ueber Verhalten und soziale Kommunikation: psychometrische Eigenschaften eines Autismus-Screening-Instruments fuer Forschung und Praxis. Diagnostica 2000; 46: 149-155.

Brian JA, Bryson SE. Disembedding performance and recognition memory in autism/PDD. J Child Psychol Psychiatry 1996; 37: 865-872.

Brown C, Gruber T, Boucher J, Rippon G, Brock J. Gamma abnormalities during perception of illusory figures in autism. Cortex 2005; 41: 364-376.

Bruning N, Konrad K, Herpertz-Dahlmann B. Bedeutung und Ergebnisse der Theory of Mind-Forschung für den Autismus und andere psychiatrische Erkrankungen. Z Kinder Jugendpsychiatr Psychother. 2005; 33:77-88.

Buccino G, Binkofski F, Fink GR, Fadiga L, Fogassi L, Gallese V, Seitz RJ, Zilles K, Rizzolatti G, Freund HJ. Action observation activates premotor and parietal areas in a somatotopic manner: an fMRI study. European Journal of Neuroscience 2001; 13: 400-404.

Büchel C, Friston KJ. Modulation of connectivity in visual pathways by attention: cortical interactions evaluated with structural equation modelling and fMRI. Cerebral Cortex 1997;7:768-778.

Chakrabarti S, Fombonne E. Pervasive developmental disorders in preschool children. J. Am. Medical Association 2001; 285: 3093-3099.

Chez MG, Aimonovitch M, Buchanan T, Mrazek S, Tremb RJ. Treating autistic spectrum disorders in children: utility of the cholinesterase inhibitor rivastigmine tartrate. J Child Neurol 2004; 19: 165-169.

Cobrinik L. The performance of brain-injured children on hidden-figures tasks. Am J Psychol 1959; 72: 566-571.

Cody H, Pelphrey K, Piven J. Structural and functional magnetic resonance imaging of autism. Int J Dev Neurosci 2002; 20: 421-438.

Corbetta M, Shulman G, Miezin FM, and Petersen SE. Superior parietal cortex activation during spatial attention shifts and visual feature conjunction. Science 1995; 270: 802-805.

Corbetta M, Shulman GL. Human cortical mechanisms of visual attention during orienting and search. Phil Trans Roy Soc Lond B 353: 1353-1362.

Corbetta M, Kincade JM, Ollinger JM, McAvoy MP, Shulman GL. Voluntary orienting is dissociated from target detection in human posterior parietal cortex. Nature Neuroscience 2000, 3: 292-297.

Corkin S. Hidden-figures-test performance: lasting effects of unilateral penetrating head injury and transient effects of bilateral cingulotomy. Neuropsychologia 1979; 17: 585-605.

Courchesne E, Redcay E, Morgan JT, Kennedy DP. Autism at the beginning: microstructural and growth abnormalities underlying the cognitive and behavioral phenotype of autism. Dev Psychopathol 2005; 17:577-597.

Dawson G, Webb SJ, McPartland J. Understanding the nature of face processing impairment in autism: insights from behavioral and electrophysiological studies. Dev Neuropsychol 2005; 27: 403-424.

Doyon J, Milner B. Right temporal-lobe contribution to global visual processing. Neuropsychologia 1991; 29: 343-360.

Eickhoff SB, Stephan KE, Mohlberg H, Grefkes C, Fink GR, Amunts K, Zilles K. A new SPM toolbox for combining probabilistic cytoarchitectonic maps and functional imaging data. Neuroimage 2005; 25: 1325-1335.

Fink GR, Dolan RJ, Halligan PW, Marshall JC, and Frith CD. Space-based and object-based visual attention: shared and specific neural domains. Brain 1997a; 120: 2013-2028.

Fink GR, Driver J, Rorden C, Baldeweg T, Dolan RJ. Neural consequences of competing stimuli in both visual hemifields: a physiological basis for visual extinction. Ann Neurol 2000; 47: 440-446.

Fink GR, Halligan PW, Marshall JC, Frith CD, Frackowiak RSJ, Dolan RJ. Where in the brain does visual attention select the forest and the trees? Nature 1996; 382: 626-628.

Fink GR, Halligan PW, Marshall JC, Frith CD, Frackowiak RSJ, and Dolan RJ. Neural mechanisms involved in the processing of global and local aspects of hierarchically organized visual stimuli. Brain 1997b ;120: 1779-1791.

Fink GR, Marshall JC, Shah NJ, Weiss PH, Halligan PW, Grosse-Ruyken M, Ziemons K, Zilles K, Freund HJ. Line bisection judgments implicate right parietal cortex and cerebellum as assessed by fMRI. Neurology 2000; 54:1324-1331.

Fink GR, Marshall JC, Weiss PH, Zilles K. The neural basis of vertical and horizontal line bisection judgments: an fMRI study of normal volunteers. NeuroImage 2001; 14: 59-67.

Folstein SE, Rosen-Sheidley B. Genetics of autism: complex aetiology for a heterogeneous disorder. Nat Rev Genet 2001; 2: 943-955.

Fombonne E. The prevalence of autism. JAMA 2003; 289(1): 87-89.

Friston KJ. Functional and effective connectivity: A synthesis. Human Brain Mapping 1994; 2: 56-78.

Friston KJ, Ashburner J, Frith CD, Poline JB, Heather JD, and Frackowiak RSJ. Spatial registration and normalization of images. Hum Brain Mapp 1995a ; 3: 165-189.

Friston KJ, Holmes A, Worsley KJ, Poline JB, Frith CD, and Frackowiak RSJ. Statistical parametric maps in functional imaging: a general linear approach. Hum Brain Mapp 1995b; 2: 189-210.

Friston KJ, Büchel C, Fink GR, Morris J, Rolls E, Dolan RJ. Psychophysiological and modulatory interactions in neuroimaging. NeuroImage 1997; 6: 218-229.

Friston KJ. Imaging neuroscience: principles or maps? Proceedings of the National Academy of Sciences U. S. A. 1998; 95: 796-802.

Friston KJ, Holmes AP, Worsley KJ. How many subjects constitute a study? NeuroImage 1999; 10: 1-5.

Friston KJ. The labile brain. I. Neuronal transients and nonlinear coupling. Philosophical Transactions of the Royal Society of London B: Biological Sciences 2000; 355: 215-236.

Friston KJ. Functional integration and inference in the brain. Progress in Neurobiology 2002; 68: 113-143.

Friston KJ, Price CJ. Degeneracy and redundancy in cognitive anatomy. Trends in Cognitive Sciences 2003; 7: 151-152.

Friston KJ, Harrison L, Penny W. Dynamic causal modeling. NeuroImage 2003, 19 1273-1302.

Frith U. Autism: Explaining the enigma. Blackwell Science; 1989.

Frith U, Happe F. Autism spectrum disorder. Curr Biol 2005; 15: R786-90.

Gillberg C, Colemann M. The biology of the autistic syndromes. 3rd edition London: Mac Keith Press 2000.

Gilchrist A, Green J, Cox A, Burton D, Rutter M, Le Couteur A. Development and current functioning in adolescents with Asperger syndrome: a comparative study. J Child Psychol Psychiatry 2001; 42: 227-40.

Gitelman DR, Bernero J, and Ray R. ILAB: a program for analyzing eye movements. 2001

Gitelman DR, Parrish TB, Friston KJ, Mesulam MM. Functional anatomy of visual search: regional segregations within the frontal eye fields and effective connectivity of the superior colliculus. NeuroImage 2002, 15: 970-982.

Glasson EJ, Bower C, Petterson B, de Klerk N, Chaney G, Hallmayer JF. Perinatal factors and the development of autism: a population study. Arch Gen Psychiatry 2004; 61: 618–627.

Gottesman I, Gould TD. The endophenotype concept in psychiatry: etymology and strategic intentions. Am J Psychiatry 2003; 160: 636-645.

Gottschaldt K. Über den Einfluss der Erfahrung auf die Wahrnehmung von Figuren, I. Psychol Forsch 1926; 8: 261-317.

Gottschaldt K. Über den Einfluss der Erfahrung auf die Wahrnehmung von Figuren, II. Psychol Forsch 1929:12: 1-87.

Happé FGE. Autism: An introduction to psychological theory. UCL Press, London. 1994

Happé FGE. An advanced test of theory of mind: understanding of story characters' thoughts, and feelings by able autistic, mentally handicapped, and normal children and adults. J Autism Devl Disorder 1994; 24: 129–154.

Happé FGE. Studying weak central coherence at low levels: children with autism do not succumb to visual illusions: a research note. J Child Psychol Psychiatry 1996; 37: 873–877.

Happé FGE. Central coherence and theory of mind in autism: reading homographs in context. Br J Dev Psychol 1996; 15: 1-12.

Happé F. Understanding assets and deficits in autism: why success is more interesting than failure. The Psychologist 1999;12: 540-546.

Happé F, and Frith U. The neuropsychology of autism. [Review]. Brain 1996; 119: 1377-1400.

Heilman KM, Valenstein E. Clinical neuropsychology. Oxford University Press, Oxford 1993.

Herwig U, Abler B, Schonfeldt-Lecuona C, Wunderlich A, Grothe J, Spitzer M, Walter H. Verbal storage in a premotor-parietal network: evidence from fMRI-guided magnetic stimulation. NeuroImage 2003; 20: 1032-1041

Hill EL, Frith U. Understanding autism: insights from mind and brain. Philos Trans R Soc Lond B Biol Sci 2003; 358: 281-289.

Hopfinger JB, Buonocore MH, Mangun GR. The neural mechanisms of top-down attentional control. Nature Neuroscience 2000; 3: 284-291.

Iacoboni M, Woods RP, Brass M, Bekkering H, Mazziotta JC, Rizzolatti G. Cortical mechanisms of human imitation. Science 1999; 286: 2526-2528.

Jambaque I, Mottron L, Ponson G, and Chiron C. Autism and visual agnosia in a child with right occipital lobectomy. J Neurol Neurosurg Psychiatr 1998; 65: 555-560.

Jollife T, and Baron-Cohen S. Are people with autism and Asperger syndrome faster than normal on the Embedded Figures Test? J Child Psychol Psychiatry 1997;38: 527-534.

Kagan J, Kogan N. Individual variation in cognitive processes. In: P. Mussen, editor. Carmichael's Manual of Child Psychology. New York: Wiley; 1970; 1: 1273-1365.

Kanner L, Autistic disturbances of affective contact. Nervous Child 1943; 2: 217-250

Kemper TL, Bauman M. Neuropathology of infantile autism. J Neuropathol Exp Neurol 1998; 57: 645-652.

Kim YH, Gitelman DR, Nobre, AC, Parrish TB, LaBar KS, Mesulam MM. The large-scale neural network for spatial attention displays multifunctional overlap but differential asymmetry. NeuroImage 1999; 9: 269-277.

Kötter R, Stephan KE. Network participation indices: characterizing component roles for information processing in neural networks. Neural Networks 2003, 16(9): 1261-1275.

Lamb JA, Moore J, Bailey A, Monaco AP. Autism: Recent molecular genetic advances. Human Molecular Genetics 2000; 9: 861-868.

Lord C, Risi S, Lambrecht L, Cook EH, Leventhal B, DiLavore PC, Pickels A, Rutter M. The ADOS-G (Autism Diagnostic Observation Schedule-Generic): A standard measure of social-communication deficits associated with autism spectrum disorders. J Autism Devl Disorder 2000; 30:205-223.

Macaluso E, Frith CD, Driver J. Modulation of human visual cortex by crossmodal spatial attention. Science 2000; 289: 1206-1208.

Manjaly ZM, Marshall JC, Stephan KE, Gurd JM, Zilles K, Fink GR. In search of the hidden: an fMRI study with implications for the study of patients with autism and with acquired brain injury. NeuroImage 2003; 19: 674-683.

Manjaly ZM, Marshall JC, Stephan KE, Gurd JM, Zilles K, Fink GR. Context-dependent interactions of left posterior inferior frontal gyrus in a local visual search task unrelated to language. Cognitive Neuropsychology 2005; 22: 292-305

Manjaly ZM, Bruning N, Neufang S, Stephan KE, Brieber S, Marshall JC, Kamp-Becker I, Remschmidt H, Herpertz-Dahlmann B, Konrad K, Fink GR. Neurophysiological correlates of relatively enhanced local visual search in autistic adolescents. NeuroImage 2007, 35: 283-291.

Marshall JC, Fink GR. Spatial cognition: where we were and where we are. NeuroImage 2001; 14: 2-7.

Mayes SD, Calhoun SL, Crites DL. Does DSM-IV Asperger's disorder exist? Journal of Abnormal Child Psychology 2001; 29: 263-271.

McAlonan GM, Cheung V, Cheung C, Suckling J, Lam GY, Tai KS, Yip L, Murphy DG, Chua SE. Mapping the brain in autism. A voxel-based MRI study of volumetric differences and intercorrelations in autism. Brain 2005; 128: 268-276.

McIntosh AR. Towards a network theory of cognition. Neural Networks 2000;13: 861-870.

McIntosh AR, Rajah MN, Lobaugh NJ. Functional connectivity of the medial temporal lobe relates to learning and awareness. Journal of Neuroscience 2003; 23: 6520-6528.

McPartland J, Dawson G, Webb SJ, Panagiotides H, Carver LJ. Event-related brain potentials reveal anomalies in temporal processing of faces in autism spectrum disorder. J Child Psychol Psychiatry 2004; 45: 1235-1245.

Miller J, and Navon D. Global precedence and response activation: evidence from LRPs. Q-J-Exp-Psychol-A 2002; 55A: 289-310.

Mottron L, Burack JA, Stauder JEA, and Robaey P. Perceptual processing among high-funcitoning persons with autism. J Child Psychol Psychiatry 1999; 40: 203-211.

Mottron L, Burack JA, Iarocci G, Belleville S, Enns JT. Locally oriented perception with intact global processing among adolescents with high-functioning autism: evidence from multiple paradigms. J Child Psychol Psychiatry 2003; 44: 904-913.

Nichols T, Brett M, Andersson J, Wager T, Poline JB. Valid conjunction inference with the minimum statistic. Neuroimage 2005; 25: 653-660.

Nishitani N, Hari R. Temporal dynamics of cortical representation for action. Proceedings of the National Academy of Sciences U. S. A 2000; 97: 913-918.

Orgass B, Poeck K, Kirchensteiner M, and Hartje W. Visuo-cognitive performances in patients with unilateral hemispheric lesions. An investigation with three factorial reference tests. Z Neurol 1972; 202: 177-195.

O'Riordan M, Plaisted K. Enhanced discrimination in autism. Q J Exp Psychol A 2001; 54:961-979.

Ozonoff S, Pennington B F, Rogers SJ. Executive function deficits in high-functioning autistic individuals: relationship to theory of mind. J Child Psychol Psychiatry 1991; 32: 1081–1105.

Ozonoff S, Strayer DL, McMahon WM, Filloux F. Executive function abilities in autism and Tourette syndrome: an information processing approach. J Child Psychol Psychiatry 1994; 35: 1015-1032.

Palmer SE. Vision science: Photons to phenomenology. MIT Press, Massachusetts 1999.

Passingham RE, Stephan KE, Kötter R. The anatomical basis of functional localization in the cortex. Nature Reviews Neuroscience 2002; 3: 606-616.

Pellock JM (2004) Understanding co-morbidities affecting children with epilepsy. Neurology 2004; 62:S17-23.

Penny W, Holmes A. Random-effects analysis. In: Frackowiak RSJ, Friston KJ, Frith CD, Dolan RJ, Price CJ, Zeki S, Ashburner J, Penny W editors. Human brain function. London: Academic Press;2004; pp. 843-850.

Pierce K, Muller RA, Ambrose J, Allen G, Courchesne E. Face processing occurs outside the fusiform 'face area' in autism: evidence from functional MRI. Brain 2001; 124: 2059-2073.

Plaisted K, O'Riordan M, Baron-Cohen S. Enhanced discrimination of novel, highly similar stimuli by adults with autism during a perceptual learning task. J Child Psychol Psychiatry 1998; 39: 765-775.

Plaisted K, Swettenham J, Rees L. Children with autism show local precedence in a divided attention task and global precedence in a selective attention task. J Child Psychol Psychiatry 1999; 40: 733-742.

Plaisted K, Saksida L, Alcantara J, Weisblatt E. Towards an understanding of the mechanisms of weak central coherence effects: experiments in visual configural

learning and auditory perception. Philos Trans R Soc Lond B Biol Sci 2003; 358: 375-386.

Poldrack RA, Wagner AD, Prull MW, Desmond JE, Glover GH, Gabrieli JD. Functional specialization for semantic and phonological processing in the left inferior prefrontal cortex. NeuroImage 1999; 10: 15-35.

Polin JB, Worsley KJ, Evans AC, Friston KJ. Combining spatial extent and peak intensity to test for activations in functional imaging. NeuroImage 1997; 5: 83-96.

Price CJ, Friston KJ. Cognitive conjunction: a new approach to brain activation experiments. NeuroImage 1997; 5: 261-270.

Price CJ, Friston KJ. Degeneracy and cognitive anatomy. Trends in Cognitive Sciences 2002, 6: 416-421.

Reed SK, Angaran AJ. Structural models and embedded-figure difficulty for normal and retarded children. Perc Mot Skills 1972; 35: 155-164.

Rinehart NJ, Bradshaw JL, Moss SA, Brereton AV, Tonge BJ. Atypical interference of local detail on global processing in high-functioning autism and Asperger's disorder. J Child Psychol Psychiatry 2000; 41: 769-778.

Ring HA, Baron-Cohen S, Wheelwright S, Williams SCR, Brammer M, Andrew C., Bullmore ET. Cerebral correlates of perserved cognitive skills in autism. A functional MRI study of Embedded Figures Task performance. Brain 1999;122: 1305-1315.

Rizzolatti G, Arbib MA. Language within our grasp. Trends in Neuroscience 1998; 21: 188-194.

Rizzolatti G, Fogassi L, Gallese V. Neurophysiological mechanisms underlying the understanding and imitation of action. Nature Reviews Neuroscience 2001; 2: 661-670.

Robertson LC, Lamb, MR, Knight RT. Effects of lesions of temporal-parietal junction on perceptual and attentional processing in humans. Journal of Neuroscience 1988; 8: 3757-3769.

Ropar D, Mitchell P. Susceptibility to illusions and performance on visuospatial tasks in individuals with autism. J Child Psychol Psychiatry 2001; 42: 539-549.

Rowe JB, Stephan KE, Friston KJ, Frackowiak RJS, Lees A, Passingham RE. Attention to action in Parkinson's disease: impaired effective connectivity among frontal cortical regions. Brain 2002; 125: 276-289.

Russo M, Vignolo LA. Visual figure-ground discrimination in patients with unilateral cerebral disease. Cortex 1967; 3: 113-127.

Schultz RT, Gauthier I, Klin A, Fulbright RK, Anderson AW, Volkmar F, Skudlarski P, Lacadie C, Cohen DJ, Gore JC. Abnormal ventral temporal cortical activity during face discrimination among individuals with autism and Asperger syndrome. Arch Gen Psychiatry 2000; 57: 331-340.

Shah A, Frith U. An islet of ability in autistic children: a research note. J Child Psychol Psychiatry 1983; 24: 613-620.

Stephan KE, Marshall JC, Friston KJ, Rowe JB, Ritzl A, Zilles K, Fink GR. Lateralized cognitive processes and lateralized task control in the human brain. Science 2003; 301: 384-386.

Talairach J, Tournoux P. Co-planar stereotactic atlas of the human brain. Thieme, Stuttgart 1988.

Tagamets MA, Horwitz B. Integrating electrophysiological and anatomical experimental data to create a large-scale model that simulates a delayed match-to-sample human brain imaging study. Cerebral Cortex 1998, 8: 310-220.

Teuber H-L, Weinstein S. Ability to discover hidden figures after cerebral lesions. Arch Neurol Psychiatry 1956; 76: 369-379.

Thiel CM, Zilles K, Fink GR. Nicotine modulates reorienting of visuospatial attention and neural activity in human parietal cortex. Neuropsychopharmacology 2005; 4: 810-820.

Tidmarsh L, Volkmar F. Diagnosis and Epidemiology of Autism Spectrum Disorders. Can J Psychiatry 2003; 48: 517-525.

Tononi G ,Sporns O, Edelman GM. Measures of degeneracy and redundancy in biological networks. Proceedings of the National Academy of Sciences U. S. A. 1999; 96 3257-3262.

Volkmar F, Pauls D. Autism. Lancet 2003; 362:1133-1141.

Weber B, Schwarz U, Kneifel S, Treyer V, Buck A. Hierarchical visual processing is dependent on the oculomotor system. Neuroreport 2000; 11: 241-247.

Yantis S, Schwarzbach J, Serences JT, Carlson RL, Steinmetz MA, Pekar JJ, Courtney SM. Transient neural activity in human parietal cortex during spatial attention shifts. Nature Neuroscience 2002; 5: 995-1002.

Weiß RH. Grundintelligenztest Skala 2 (CFT 20) mit Wortschatztest (WS) und Zahlenfolgentest (ZF). 4th edition. Braunschweig: Westermann; 1998.

Wellman HM, Baron-Cohen S, Caswell R, Gomez JC, Swettenham J, Toye E, Lagattuta K. Thought-bubbles help children with autism acquire an alternative to a theory of mind. Autism 2002; 6: 343-363.

Wiznitzer M. Autism and tuberous sclerosis. J Child Neurol 2004; 19: 675-679.

World Health Organization. The ICD-10 classification of mental and behavioural disorders: diagnostic criteria for research. Geneva: World Health Organization; 1993.

Young MP, Hilgetag CC, Scannell JW. On imputing function to structure from the behavioural effects of brain lesions. Philosophical Transactions of the Royal Society of London B: Biological Sciences 2000; 355:147-161.

5. Zusammenfassung in deutscher Sprache

Autismus und die Theorie der schwachen zentralen Kohärenz: Untersuchungen mit funktioneller Magnetresonanztomographie

Eine Vielzahl früherer Studien deutet darauf hin, dass Autisten bei verschiedenen visuellen Aufgaben überlegene Leistungen aufweisen, wenn es darum geht, lokale Details des visuellen Stimulus zu verarbeiten. Ein bekanntes Beispiel dafür ist der sogenannte "Embedded Figures Task" (EFT). Bei diesem neuropsychologischen Test bekommen die Testpersonen jeweils zwei visuelle Stimuli parallel gezeigt, eine komplexe geometrische Form und eine kleinere, einfache Form. Die Aufgabe besteht darin, so schnell wie möglich zu entscheiden, ob die einfache Form in der komplexen enthalten ist oder nicht. Bei diesem Test ist es hilfreich, wenn man die Gesamtform (den "globalen Kontext") ignorieren kann und stattdessen vornehmlich die lokalen Elemente wahrnimmt. Autisten weisen bei diesem Test gegenüber Kontrollpersonen in vielen Studien überlegene Leistungen auf.

Dieses Phänomen. d.h. Übergewichtung lokaler Information und relative Vernachlässigung globaler Information, ist als "schwache zentrale Kohärenz" bekannt. Schwache zentrale Kohärenz ist ein kognitiver Mechanismus, mit dem sich viele der psychologischen Auffälligkeiten bei autistischen Patienten potentiell erklären lassen. Wenngleich eine Vielzahl von psychologischen Studien zur schwachen zentralen Kohärenz durchgeführt wurden, ist bislang wenig über die zugrundeliegenden neurophysiologischen Mechanismen bekannt. Das Wissen um diese neuronale Grundlage ist jedoch notwendig, um die Pathophysiologie des Autismus zu verstehen und letztendlich effektive Therapien zu entwickeln. Aus diesen Gründen untersuchte ich in meiner medizinischen Doktorarbeit bei Prof. Dr. Gereon Fink (Neurologische Klinik, RWTH Aachen & Institut für Medizin,

Forschungszentrum Jülich) die neuronalen Korrelate der Wahrnehmung lokaler Details im EFT mittels funktioneller Magnetresonanztomographie (fMRT), und inwiefern sich diese Korrelate bei autistischen Jugendlichen und Kontrollpersonen unterscheiden.

Obwohl der EFT seit längerer Zeit ein populäres Verfahren zur psychologischen Untersuchung von Autisten ist, war bislang weitgehend unbekannt, auf welchen neurophysiologischen Mechanismen die von ihm erforderte lokale visuelle Wahrnehmung eigentlich beruht. In einer ersten Studie untersuchte ich deshalb, welche Hirnregionen gesunder Erwachsener entscheidend für die Wahrnehmung lokaler Details bei der Durchführung des EFT sind (Manjaly et al. 2003, NeuroImage 19: 674-683). Zu diesem Zweck entwickelte ich eine fMRT-kompatible Version des EFT, die mehrere geeignete Kontrollbedingungen enthielt. Erst durch diese Kontrollbedingungen war es möglich, diejenigen Areale zu bestimmen, die spezifisch für die Wahrnehmung lokaler Details in komplexen visuellen Stimuli verantwortlich sind. In der Analyse der gemessenen fMRT-Daten von 16 gesunden erwachsenen Freiwilligen fanden sich zwei Areale, die eine solche spezifische Rolle besassen: der linke inferiore frontale Gyrus (IFG), auch als "Broca-Areal" bekannt, und der linke intraparietale Sulcus (IPS). An diesem Resultat sind zwei Aspekte bemerkenswert. Erstens, dass beide Areale in der linken Hirnhälfte liegen. Dieser Befund bestätigt frühere psychologische Arbeiten, die nahelegten, dass die linke Hirnhälfte eine Spezialisierung für die Verarbeitung lokaler Information zeigt, während die rechte Hirnhälfte für die Prozessierung globaler Information spezialisiert ist. Zweitens war die Beteiligung des sprachrelevanten Broca-Areals an lokalen visuellen Wahrnehmungsprozessen eine Überraschung. Es gab zwei Möglichkeiten, die bekannte Rolle des Broca-Areals für Sprachverarbeitung und –produktion mit unserem Ergebnis in Einklang zu bringen: entweder der EFT kann mit Hilfe

sprachbasierter kognitiver Strategien durchgeführt werden oder die häufig gemachte Annahme, dass bestimmte Hirnregionen eine fixe Beziehung zu bestimmten mentalen Funktionen aufweisen, ist zu stark. In der Tat mehren sich Befunde, die darauf hindeuten, dass kognitive Funktionen aus der Interaktion multipler Hirnareale resultieren, und diese Kopplungen zur Ausbildung temporärer und kontext-sensitiver funktioneller Netzwerke führen. In anderen Worten, Hirnregionen verändern ihre Interaktionen untereinander in Abhängigkeit davon, welche Funktion gerade ausgeführt werden soll.

Um zwischen diesen beiden Erklärungen zu unterscheiden, führte ich in einer zweiten Studie eine Analyse der funktionellen Interaktionen des Broca-Areals mit allen anderen Hirnregionen durch (Manjaly et al. 2005, Cognitve Neuropsychology 22: 292-305). In dieser Konnektivitätsanalyse fand ich, dass sich während des EFT die funktionelle Kopplung des Broca-Areals spezifisch mit solchen Arealen veränderte, die für ihre Beteiligung an visuell-räumlichen, nicht aber sprachlichen, Prozessen bekannt sind. Dieser Befund ist bislang einer der eindeutigsten Demonstrationen für die Kontext-Sensitivität regionaler Hirnaktivierungen und ihre Abhängigkeit davon, in welches funktionelle Netzwerk die Region sich einbinden kann. Für den EFT bedeutet dieses Resultat konkret, dass die Aktivierung des Broca-Areals im EFT tatsächlich Ausdruck einer Beteiligung an lokaler visueller Suche ist, und nicht durch den Einfluss etwaiger sprach-basierter Strategien zustande kommt.

Auf der Grundlage dieser initialen Studien konnte nun die entscheidende Frage angegangen werden: Was sind die neuronalen Mechanismen, auf denen die lokale visuelle Wahrnehmungsleistung der Autisten im EFT beruht? Zwei konkurrierende Hypothesen mussten unterschieden werden. Gemäß des klassischen Konzepts der

schwachen Kohärenz geht die überlegene lokale visuelle Wahrnehmungsleistung der Autisten zulasten der Fähigkeit, globalen Kontext wahrzunehmen. Diese Hypothese sagt voraus, dass man bei Autisten eine extreme linkshemisphärische Spezialisierung für die Analyse der im EFT verwendeten komplexen Stimuli erwarten würde, insbesondere eine noch stärkere Aktivierung im linken IFG und linken IPS als bei der gesunden Kontrollgruppe in der ersten Studie. Die alternative Hypothese ist, dass Autisten lokale Details besser aus ihrem Zusammenhang herauslösen und schneller prozessieren können, ohne dass dies zulasten der Verarbeitung globaler Information geht. Dann würde man bei ihnen eine stärkere Aktivierung primärer und sekundärer visueller Areale erwarten, die aufgrund kleiner rezeptiver Felder und damit hoher Ortsauflösung für die Prozessierung von Detailaspekten besonders befähigt sind. Diese Aktivierungen müssten aber nicht zwangsläufig allein in der linken Hemisphäre auftreten, sondern könnten auch symmetrisch vorkommen.

Um diese beiden Hypothesen gegeneinander zu testen, rekrutierten wir 12 autistische Jugendliche und untersuchten ihre Hirnaktivität während der Durchführung des EFTs. Als Kontrollgruppe dienten 12 gesunde Jugendliche, die in Geschlecht, Händigkeit, Alter und Intelligenzquotient den autistischen Patienten entsprachen. Die Analyse der fMRT-Daten ergab, dass bei den gesunden Jugendlichen ähnliche Areale aktiviert waren wie bei den gesunden Erwachsenen, d.h. intraparietale und frontale Regionen. Hingegen fand sich bei den Autisten eine erhöhte Aktivierung im primären und sekundären visuellen Kortex in beiden Hemisphären (Manjaly et al. 2007, NeuroImage 35: 283-291).

Dieses Ergebnis spricht für die zweite Hypothese: Bei Autisten scheint die überlegene visuelle Prozessierung lokaler Detailaspekte nicht zulasten der Verarbeitung globalen Kontexts zu verlaufen. Allerdings zeigte eine statistische

Analyse der Verhaltensdaten auch, dass Autisten zwar einen *relativen* Leistungsvorteil beim EFT hatten (d.h. ihre EFT-Leistungen waren im Vergleich zu Kontrolltests besser als bei den gesunden Probanden), nicht aber eine *absolute* Überlegenheit aufwiesen. Nach unseren Ergebnissen sind Autisten also nicht absolut besser bei der Analyse lokaler Detailinformation in visuellen Stimuli, aber sie führen diese Analyse anders durch als gesunde Testpersonen. Diese kognitive Andersartigkeit scheint durch Funktionsunterschiede des primären und sekundären visuellen Kortex bedingt zu sein.

6. Acknowledgments

I would like to thank those people who, through their support and advice, have made this work possible.

First of all, I am particularly grateful to Prof. Dr. Gereon R. Fink who has been a fantastic supervisor for me. Over the years, he has given me enormous support and encouragement for every aspect of my work and my general scientific education.

I would also like to thank Prof. Dr. Karl Zilles for his support. It was him who recommended me to Prof. Fink.

Words can hardly express how grateful I am to Dr. Klaas Enno Stephan. He gave me his unlimited support in every aspect and at each stage of my work and always believed in me and encouraged me.

My special thanks go to Prof. John Marshall in Oxford who has always been a great advisor, an invaluable critics and a good teacher.

I would also like to express my gratitude towards my colleagues in the Cognitive Neurology group at Jülich who, as well as my fellow researchers at the Dept. of Child and Adolescent Psychiatry at Aachen, have been very supportive and collegial.

Last, but not least, I would express my deepest thanks to my parents, Annie & Johny Manjaly, and my sister, Zita Rose. Their never-ending love, companionship and support have made me the person who I am today. There has never been a single moment in my life in which I was unsure of their love.

7. Tabellarischer Lebenslauf

- geboren am 30.10. 1980 in Duisburg als älteste Tochter von Annie und Johny Manjaly
- 1986 -1990: Katholische Grundschule Salzmannstrasse, Duisburg
- 1990 - 1999: Elly-Heuss Knapp Gymnasium, Duisburg; Abiturnote 1,6
- 1996 - 1997: Austauschjahr am Scarlett Heights Collegiate Institute, Toronto, Kanada
- 1999 - 2006: Studium der Humanmedizin an der Heinrich-Heine-Universität Düsseldorf; Approbation zur Ärztin durch das 3. medizinische Staatsexamen mit der Gesamtnote "gut"
- 2001 – 2006: Doktorandin in der Arbeitsgruppe Kognitive Neurologie am Institut für Medizin, Forschungszentrum Jülich (betreut von Prof. G.R. Fink)
- 2005 - 2006 Praktisches Jahr:
    1. Tertial: Neurologie, National Hospital of Neurology and Neurosurgery, University College London, England
    2. Tertial: Chirurgie, Northern General Hospital, University of Sheffield, England
    3. Tertial: Innere Medizin (Kardiologie), Universitätsspital Zürich, Schweiz
- 2006 – 2007: Assistenzärztin (Foundation Year 2) am Maidstone Hospital (Lehrkrankenhaus des King's College London), mit Ausbildung in Innerer Medizin, Notfallmedizin und Psychiatrie
- ab September 2007: Assistenzärztin in Neurologie am Unispital Zürich
- Stipendien & Auszeichnungen:
    - 2004 - 2006: Stipendiatin der Studienstiftung des deutschen Volkes
    - 2005: Verleihung des internationalen Wissenschaftspreises "NRW Undergraduate Science Award" durch das Land Nordrhein-Westfalen
    - 2006: Verleihung des Günther-Leibfried-Preises (2. Platz) durch das Forschungszentrum Jülich
- Forschungsaufenthalte im Ausland:
    - 2003: Forschungsaufenthalt in der Clinical Neuropsychology Group der University of Oxford, England (betreut von von Dr. Jennifer Gurd & Prof. John Marshall)
    - 2005: Forschungsaufenthalt am Institute of Cognitive Neuroscience, University College London, England (betreut von Frau Professor Uta Frith)

Forschungszentrum Jülich
in der Helmholtz-Gemeinschaft

Jül-4256
Oktober 2007
ISSN 0944-2952